5 LAYERED SPACE-TIME CODED TRANSMIT DIVERSITY

In Chapters 3 it was shown that space-time processing can improve uplink performance and capacity of a cellular CDMA communication systems. In particular, techniques based on multi-antenna receive diversity and beamforming were considered. In Chapter 1 it was argued that techniques to improve the downlink performance have not been developed with the same intensity to date, but is of increasing importance due to the fact that the capacity demand imposed by the projected data services, for instance internet, burdens (more heavily) the downlink channel. It is therefore of importance to find techniques that improve the downlink capacity.

Transmit diversity (see also Section 3.2) is an effective method to combat fading when multiple receive antennas are not available. Techniques such as diversity, antenna-selection, frequency-offset, phase sweeping, and delay diversity have been studied extensively in the past [46, 47, 48, 54]. Recently, space-time coding was proposed as an alternative solution for high rate data transmission in TDMA wireless communication systems [201, 202, 203, 204].

Recent studies have explored the limit of multiple antenna system performance in a Rayleigh fading environment from an information-theoretic point-of-view [104, 205, 206]. It has been shown that, with perfect receiver channel state (side) information (CSI), and independent fading between pairs of transmit-receive antennas, the situation of total capacity may be achieved.

Foschini [104] has considered a particular layered space-time architecture with the potential to achieve higher capacity. This layered architecture forms the basis for the class of orthogonal decomposable coded space-time decoders. The chapter will focus on the construction and performance evaluation of space-time coded CDMA employing multiple transmit antennas. The classification of space-time coded transmit diversity structures is illustrated in Figure 5.1. The techniques for transmit diversity suitable for CDMA can be divided into two distinct classes, CDTD and TDTD (see Sections 3.2.1.1 and 3.2.1.2). These two coded space-time transmit diversity classes will be discussed by looking at

- the suitability of classical convolutional- and turbo codes. (The application of low rate codes, including orthogonal- and super-orthogonal convolutional codes (SOCC), is also investigated); and

- extensions of the CDTD scheme to space-time turbo diversity codes, viz. turbo transmit diversity (TTD) is considered in detail in the next chapter.

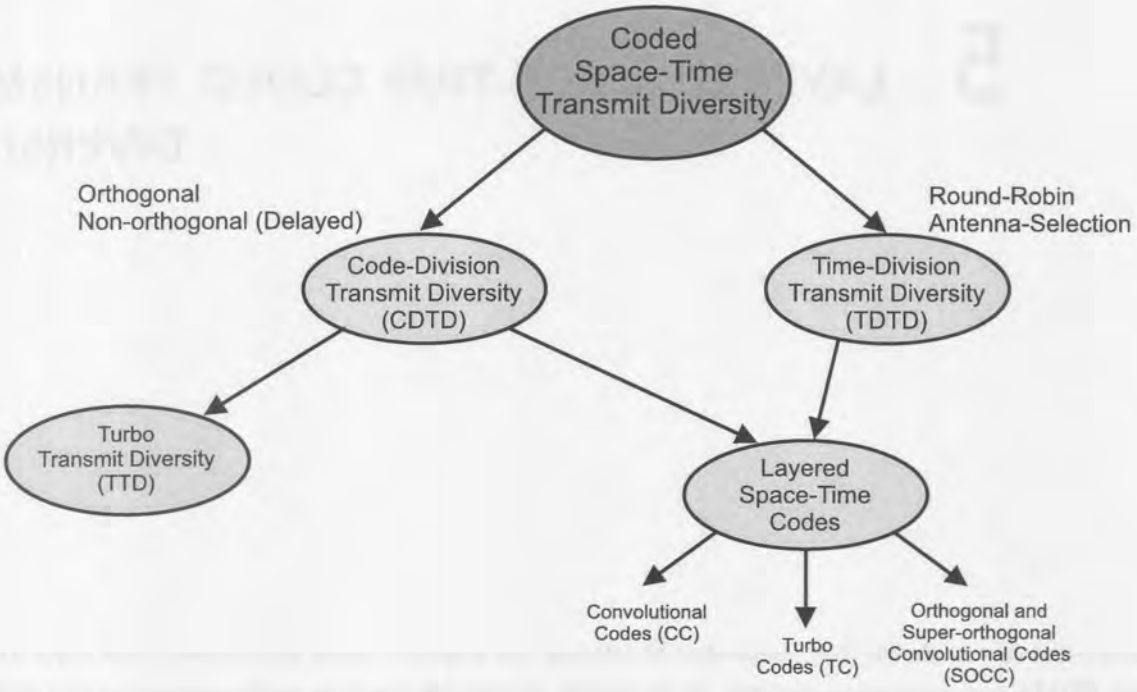

Figure 5.1. Coded transmit diversity space.

5.1 TRANSMIT DIVERSITY MULTIPLE ACCESS CHANNELS

As has been discussed earlier, the use of coded transmit diversity is an attractive solution for improving the performance and downlink capacity of CDMA communication systems.

In CDMA the channel is allocated implicitly by assigning to each information stream a unique finite length binary or non-binary (e.g., complex) signature or spreading sequence. Spreading sequences of different information streams have the same length and are almost orthogonal and, hence, messages from different users are quasi-separable by means of projections. This scheme introduces interference amongst information streams associated with different users, and this coupling between users requires a very complex receiver.

Information theoretic aspects of transmit diversity were addressed by Foschini and Gans in [206] and Telatar in [205]. Telatar derived the expressions for capacity and error exponents for multiple transmit antenna systems in the presence of Gaussian noise. Here, capacity has been derived under the assumption that the fading is statistically independent from one channel use to the other. In [206], Foschini and Gans derived the outage capacity under the assumption that the fading is quasi-static; i.e., constant over a long period of time, and then changed in an independent manner. In [104], a particular layered space-time architecture was shown to have the potential to achieve a substantial fraction of capacity.

Following the work by Urbanke [207] on multiple access communications employing coding, it is clear that the application of transmit diversity to CDMA closely resembles the classical multiple access communications problem. In the classic multiple access channel (MACH) environment there are several users competing for the available channel resources. When multiple transmit antennas are employed, the allocation of resources

is more problematic since a fair and efficient allocation of the resources among all users requires a large amount of co-ordination. This co-ordination is made more difficult by the fact that there are no direct links between the sources and the channels available and also because of the additional MAI interference.

5.1.0.1 Capacity region of transmit diversity MACH. The capacity region $\Re$ for MACHs is generally described as a polytope, i.e. a multi-dimensional figure whose faces are hyperplanes, or informal multidimensional solids with flat sides. Figure 5.2 depicts the typical region for $K \cdot M_T = 2$, the best known case since most multiple access papers focus on this special case [208].

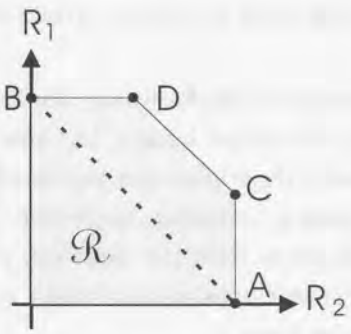

Figure 5.2. Block diagram of the dual transmit antenna single user decoder, employing an optimum successive cancellation decoder.

The reason for interest in this capacity region (besides that it is of interest in its own right) is the various operational results that follow elegantly from the particular properties of capacity region $\Re$ [207, 208]. These are described in the following.

A simple strategy to share the channel between antenna streams is time sharing. In Figure 5.2, the line AB corresponds to this scenario. Here the channel is accessed through multiple transmit antennas at disjoint moments in time, and a common time reference is needed for this scheme to work.

Following Urbanke [207], the rate tuples achievable by timesharing are those which lie on or below the line AB in Figure 5.2. The point A corresponds to the extreme case where the first transmit antenna stream of a specific user is used permanently and the second transmit antenna is never used (idle state), whereas in point B the roles of the transmit antennas are reversed. As can be seen from this example, not all points in the capacity region are achievable by means of timesharing. Hence, in order to fully utilize the given channel resources, both transmit antennas will have to access the channel concurrently. Of course, this introduces coupling among the users and, therefore, an optimum receiver (a receiver which results in the minimum achievable error probability) has to decode both users jointly. This results in high decoding complexity. Of special importance are the vertices C and D shown in Figure 5.2. It has been shown in [207], that these rate points can be achieved through *single user coding*. The latter will be addressed in more detail in the following section.

The result obtained by Wyner [209] is of particularly interest, stating that the vertices in $\Re$ are achievable by sequentially decoding one information (signature) waveform at a time. This successive decoder avoids the largest practical concern associated with multiple access communication, namely the complexity of decoders that jointly decode all waveforms at once.

This brings us to a very interesting situation. Depending on whether or not the transmitter has information on the instantaneous state of the channel, the design of space-time codes for CDMA systems can be grouped into two categories. Specifically, if the transmitter has CSI, considering the conditions of orthogonal spreading, the MACH can be decomposed into several nearly independent sub-channels. Under these conditions, the capacity region of the (frame and symbol) asynchronous MACH equals the one of the synchronous channel.

For systems in which the transmitter does not have CSI, or when the rate of information fed back from the receiver is slow, the channel cannot be decomposed as described in the foregoing. Although the lack of CSI does not imply much loss of channel capacity, the single user coding principles cannot be applied. The result is an inherently multiple space-time dimensional channel decoder, in which the redundancy embedded along the spatial as well as temporal dimensions, must be used to extract the data sources.

5.1.0.2 Single user decoding. As discussed in the foregoing, the decomposition of the MACH into independent sub-channels provides not only theoretical insight, but also potentially efficient strategies for implementing practical systems. Importantly, these strategies can be efficiently employed by a method called single user coding (also called onion peeling, stripping, successive cancellation, or superposition coding) [207, 210]. The name single user coding stems from the fact that, in the case of a dual antenna transmit scheme, the joint codeword is decoded in two steps, each of which corresponds to the decoding of a single user antenna information waveform at any time.

Consider as a special case, the single user coded dual ($M_T = 2$) antenna diversity system. The general structure for the decoder of this system is illustrated in Figure 5.3 [211].

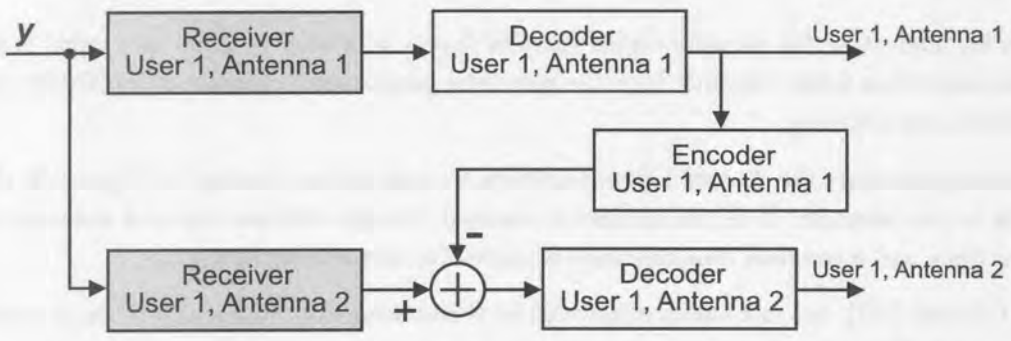

Figure 5.3. Block diagram of the dual transmit antenna single user decoder, based on optimum successive cancellation decoder.

Under these assumptions, the decoder can first decode the first antenna stream (viewing the second antenna stream as Gaussian noise). Once the correct contribution of this antenna stream is known, it can be subtracted from the received codeword and then the second antenna stream can be decoded. It has been shown in [212] that the total capacity (points C and D of Figure 5.2) can be achieved by the optimum successive cancellation decoder.

5.2 LAYERED SPACE-TIME CODES

The construction of layered space-time convolutional- and turbo coding configurations applied to multiple transmit antenna signaling is considered.

Figure 5.4 illustrates the general block diagrams of the layered space-time encoder and decoder. In this model the data source produces a sequence of N_{cc} data bits, $\mathbf{b}_k$, which enters a rate R_c encoder. The encoded sequence, $\mathbf{x}^{(j)}$ of length N_{cc}, is passed to the M_T symbol interleavers and to the multiple access transmit diversity sub-system. Recall from Figure 5.1, that this coding scenario supports both the CDTD and TDTD signalling configurations.

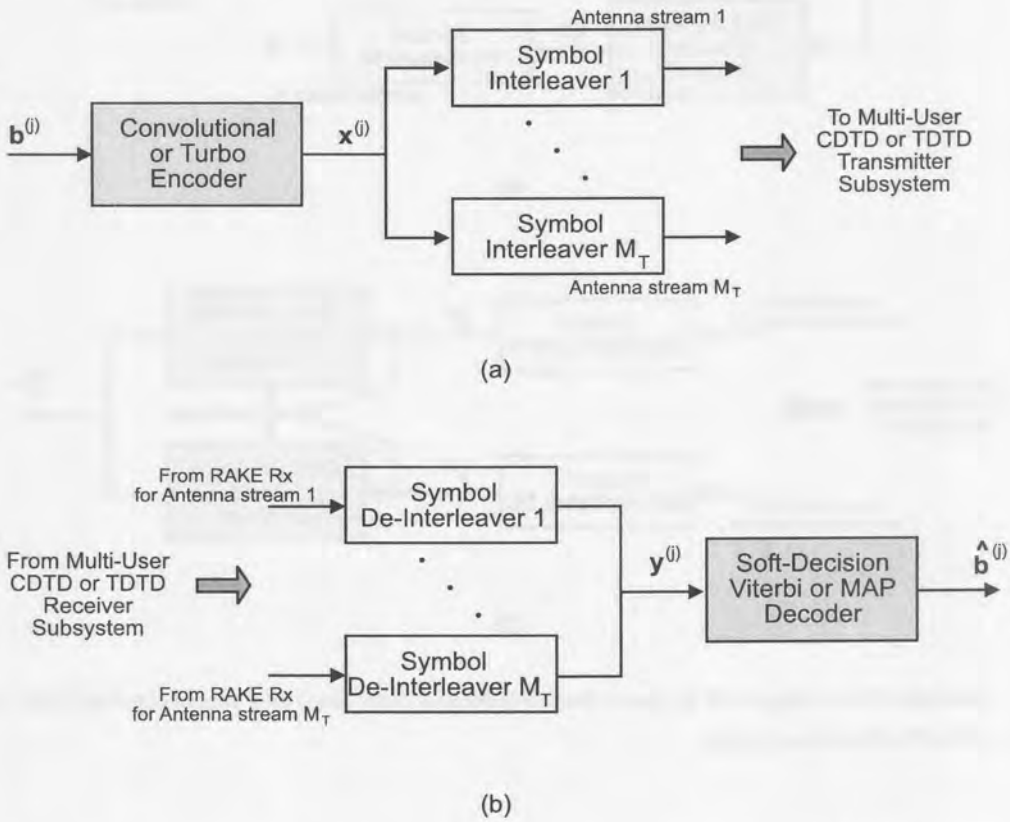

Figure 5.4. Generalized block diagram of the space-time convolutional coder based on a sub-optimum configuration. (a) Encoder, (b) Decoder.

In the receiver subsystem, the received signal is correlated with the complex scrambling/spreading sequence associated with each of the individual antenna sub-streams. With the decoding configuration, shown in Figure 5.4(b), nearly optimal decoding can be achieved by employing the Viterbi or MAP algorithm. This decoding is suboptimal since the correlator receiver is matched to the AWGN channel, and not to the MAI. It has been shown that when CSI information is available at the receiver, using soft-decision decoding and coherent detection, the coding gain on fading channels can be quite high [21].

It should be noted that for TDTD signalling, the configuration presented in Figure 5.4 can accomplish a significant portion of the theoretical system capacity, although it is a suboptimal implementation.

In contrast to the suboptimal TDTD configuration, in CDTD the M_T orthogonal streams are recovered from the receiver sub-system by means of a decorrelation process. During a specific decoding stage, the decorrelation detector only considers a single user entity for the spreading sequences associated with the M_T transmit antennas associated with the reference user. The CDTD scheme may be extended to a single user multiple antenna decoder based on a optimum successive decoder (OSD). Figure 5.5 illustrates a possible

implementation of this decoder for convolutional codes, where each user is decoded on a per-user channel basis.

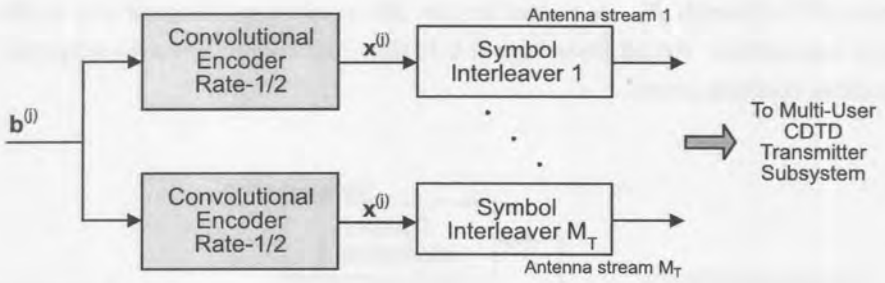

(a)

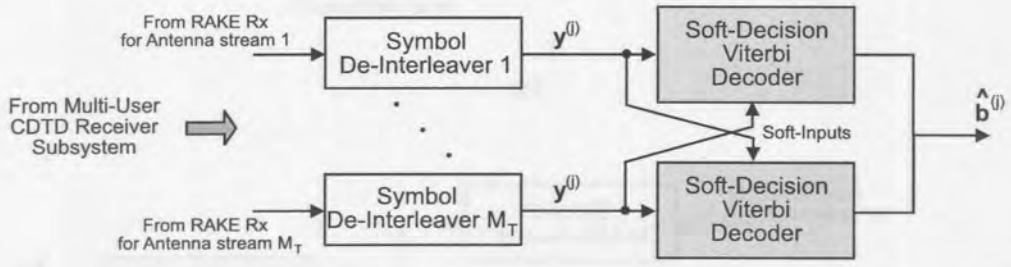

(b)

Figure 5.5. Generalized block diagram of the space-time convolutional coder based on a per-user configuration. (a) Encoder, (b) Decoder, with soft-information transfer.

In order to maintain soft failure diversity and to provide additional soft-decision information to the different decoders operating in parallel, systematic convolutional encoders are generally utilized at the encoder and decoder. In this way, the full benefits of soft-decision decoding are realized. In [211, 213], a group metric decoding scheme has been proposed that exploits the nature of the multiuser decoding problem. This decoder may be considered as a single user, single antenna decoding scheme, that will utilize information from all the user and antenna matched-filter outputs to the decoding metrics.

5.2.1 Low Rate Code Extension

The low rate codes proposed in [35, 214, 215] for CDMA, can be directly applied to configurations depicted in Figures 5.4 and 5.5. The use of orthogonal and super-orthogonal convolutional codes (SOCC) is considered.

Orthogonal block codes are known to perform well on very noisy channels. In [35], Viterbi presented a method to find orthogonal convolutional codes having similar properties. However, orthogonal convolutional codes imply a large bandwidth expansion. Along these lines, several related coding schemes with good distance properties, but less bandwidth requirements, have been proposed in [214, 215].

A rate $R_c = 1/n$ orthogonal convolutional encoder with constrained length, L_{oc}, can be constructed from a shift register and a block orthogonal encoder or signal selector [35]. One in $2^{L_{oc}}$ orthogonal waveforms is chosen based on the state of the shift register. The weight of any trellis branch (not the all-zero path)

is $2^{L_{oc}-1} = n/2$. For an orthogonal convolutional code the rate is then related to the constraint length by $R_c = 2^{L_{oc}}$. One way of implementing an orthogonal convolutional encoder is for the orthogonal code selector to choose rows from a Walsh-Hadamard matrix.

A rate $R_c = 2^{-(L_{oc}-2)}$ super-orthogonal code is obtained by modifying the orthogonal codes as follows [13]

- Let the inner $L_{oc} - 2$ stages of the shift register be used for the orthogonal waveform selection; then
- add the first and last bits of the register modulo-2 to each bit in the orthogonal waveform.

Transfer functions and upper bounds on the BEP for orthogonal and super-orthogonal convolutional codes are derived in Appendix B. Section 6.3 will consider the application of super-orthogonal turbo codes to space-time transmit diversity.

5.3 LAYERED SPACE-TIME CODES PERFORMANCE

Using (3.23), (3.29), (4.6) and the system parameters outlined in Table 5.1, the BEP performance of a cellular CDMA system employing space-time coded transmit diversity can be determined numerically.

Parameter	Simulation value
Spreading sequence length	$N = 32$
Operating environment	2-Path, equal strength.
User distribution	uniform
Number of multi-path signals	$L_p = 2$
Number of users	$K = 1, 2, \ldots, N$
Number of RAKE fingers	$L_R = 2$
Transmit diversity elements	$M_T = 1, 2, 3$
Transmit diversity technique	CDTD and AS-TDTD
FEC code type	CC and TC
FEC code rate	$R_c = 1, 1/2, \ldots, 1/6$

Table 5.1. System parameters for numerical evaluation of BEP performance.

In order to calculate the BEP of the coded CDTD and TDTD systems, the output SNR should include the transmit diversity interference term. Assuming that the cellular system is employing omni-directional antennas, the total output SNR can be determined as

$$\Gamma_{0c} = \left(\frac{1}{R_c} \frac{N_o}{2\,E_b} + \frac{(K \cdot M_T - 1)}{3N} \right)^{-1}, \tag{5.1}$$

for CDTD, and

$$\Gamma_{0c} = \left(\frac{1}{R_c} \frac{N_o}{2\,E_b} + \frac{(K - 1)}{3N} \right)^{-1}, \tag{5.2}$$

for TDTD. With reference to (3.21), it can be seen that (6.29) and (5.2) are extensions of our previous analysis and includes the code rate R_c.

It is important to note that P_e as defined in Chapter 4 represents the BEP for one spatial snapshot of the state of the cellular system. This is due to the fact that the channel model used represents one snapshot of the spatial state of the system, as described in Chapter 2. To calculate the BEP performance of the system for the average spatial state of the system P_e must be calculated a number of times and the average of these calculations determined.

5.3.1 Fading Channel Multiuser Performance

Using (4.17), (4.11) and (4.19), Figures 5.6 and 5.7 depict the BEP performance of Orthogonal CDTD (O-CDTD) under 2-path Rayleigh fast- and slow fading conditions, respectively, with rate $R_c = 1/2$ convolutional and turbo ($N_{tc} = 256, 2048$) coding. For both graphs, the number of users $K = 5$ with $M_T = 1, 2$ and 3 transmit antenna elements.

By introducing multiple transmit antennas, the diversity order is increased, and thereby the probability of coding gain is increased. This is especially true for turbo coded transmit diversity which is better suited for Gaussian-like MAI. From the graphs it clear that turbo coded transmit diversity increases the performance substantially.

Using the bounds on BEP performance derived in Section 4.2, Figures 5.8 to 5.12 depict the performance as a function of system load, V for coded O-CDTD CDMA. The analysis is restricted to a fully interleaved (i.e., fast fading) two path Rayleigh fading channel. The operating point has been taken as $E_b/N_0 = 20$ dB. Figures 5.8 and 5.9 compare coded ($R_c = 1/2$) and uncoded O-CDTD BEP performance as a function of interleaver size and transmit diversity order, with $M_T = 1, 2$. Results for single transmit diversity ($M_T = 1$) are included in an attempt to isolate the performance improvement achieved with temporal diversity from the total space-time diversity gain. From the curves it is clear that the introduction of coded transmit diversity has improved the capacity of all the coded systems quite substantially. For regions of high system load, the best performance is achieved by the turbo coded systems.

Figures 5.10 and 5.11 compare the performance of different low code rates and transmit diversity order, $M_T = 1, 2$. For the turbo coded systems the interleaver size was 256. The low rate codes provide improved performance over the complete range. This illustrates the effectiveness of low rate codes to overcome loss in processing gain under equal bandwidth conditions.

Figure 5.12 compares the performance of coded O-CDTD with $R_c = 1/2$ and transmit diversity order, $M_T = 1, 3$. From the graphs it can be seen that the best performance is always achieved with the highest order diversity.

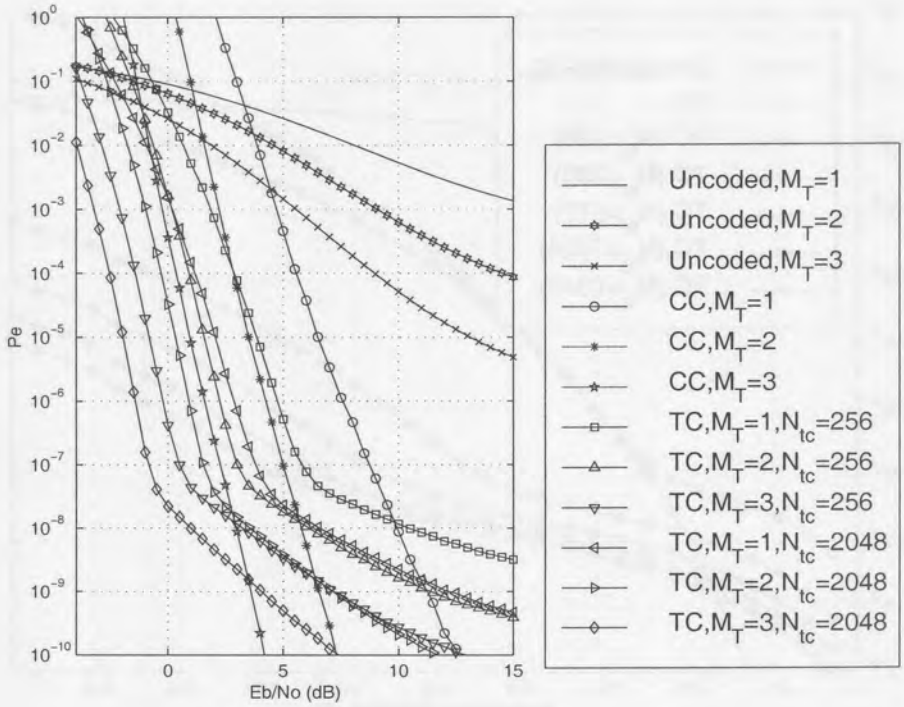

Figure 5.6. Analytical BEP performance of coded O-CDTD, with $R_c = 1/2$, $K = 5$, and $M_T = 1, 2, 3$, on a fast fading 2-path channel.

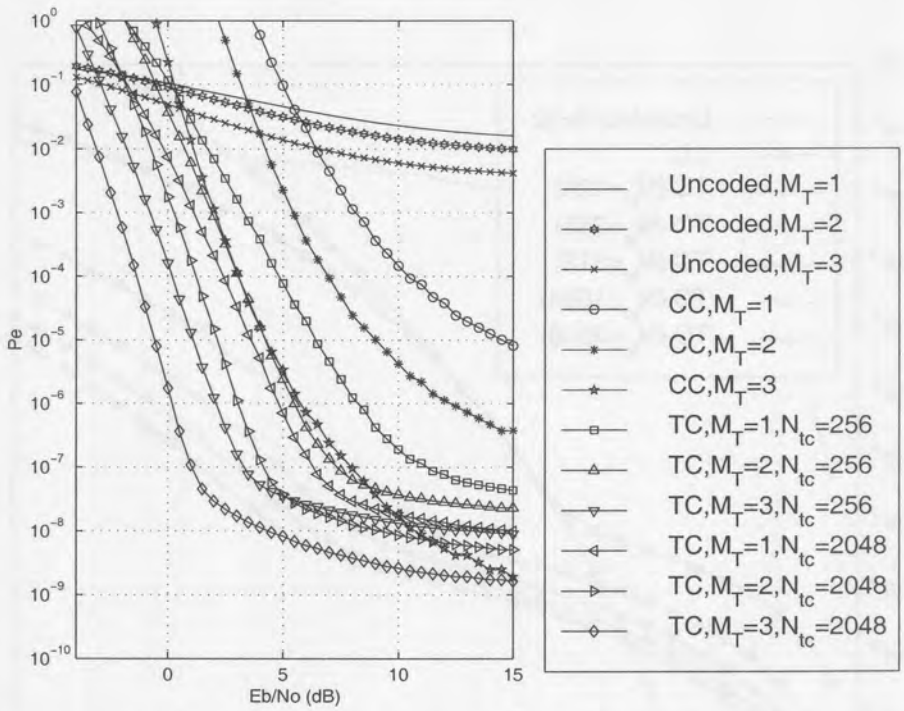

Figure 5.7. Analytical BEP performance of coded O-CDTD, with $R_c = 1/2$, $K = 5$, and $M_T = 1, 2, 3$, on a slow fading 2-path channel.

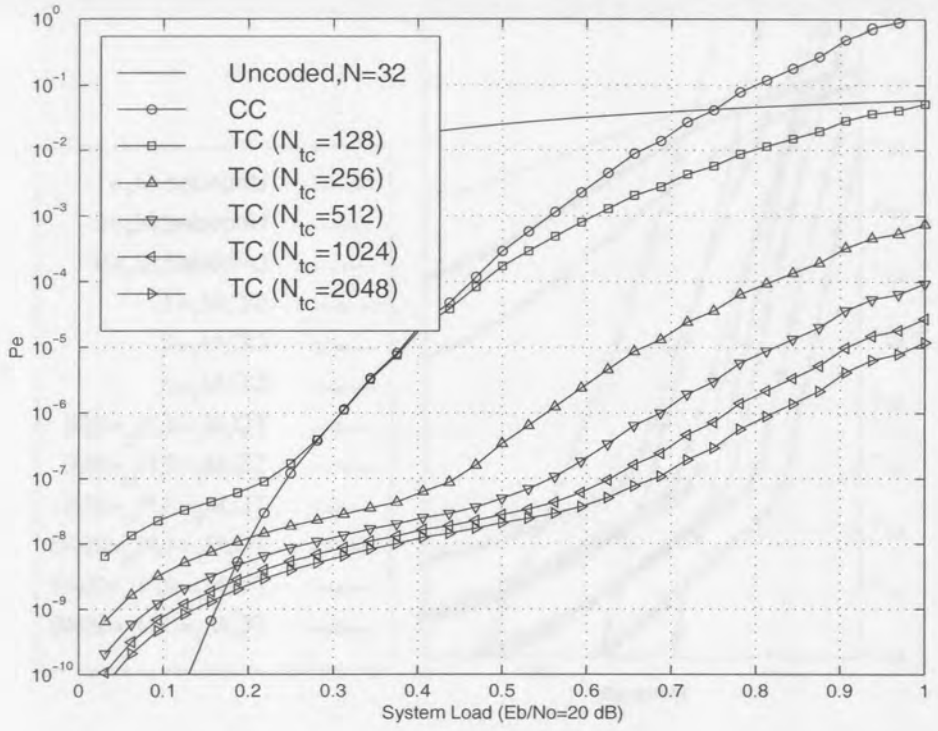

Figure 5.8. Coded O-CDTD BEP performance on a 2-path fading channel with $R_c = 1/2$ and $M_T = 1$.

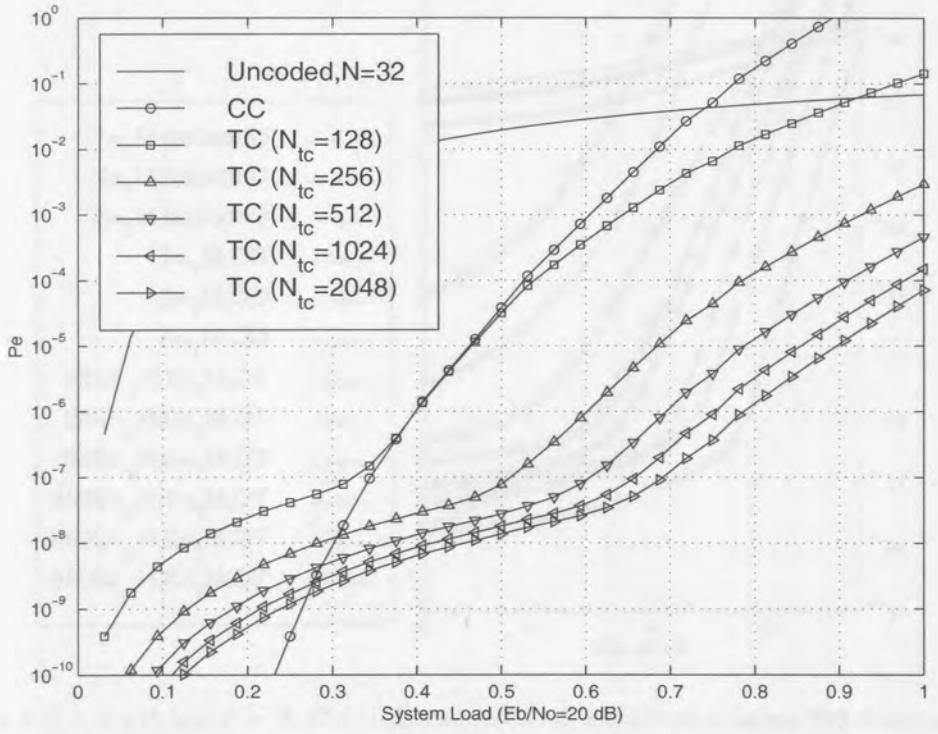

Figure 5.9. Coded O-CDTD BEP performance on a 2-path fading channel with $R_c = 1/2$ and $M_T = 2$.

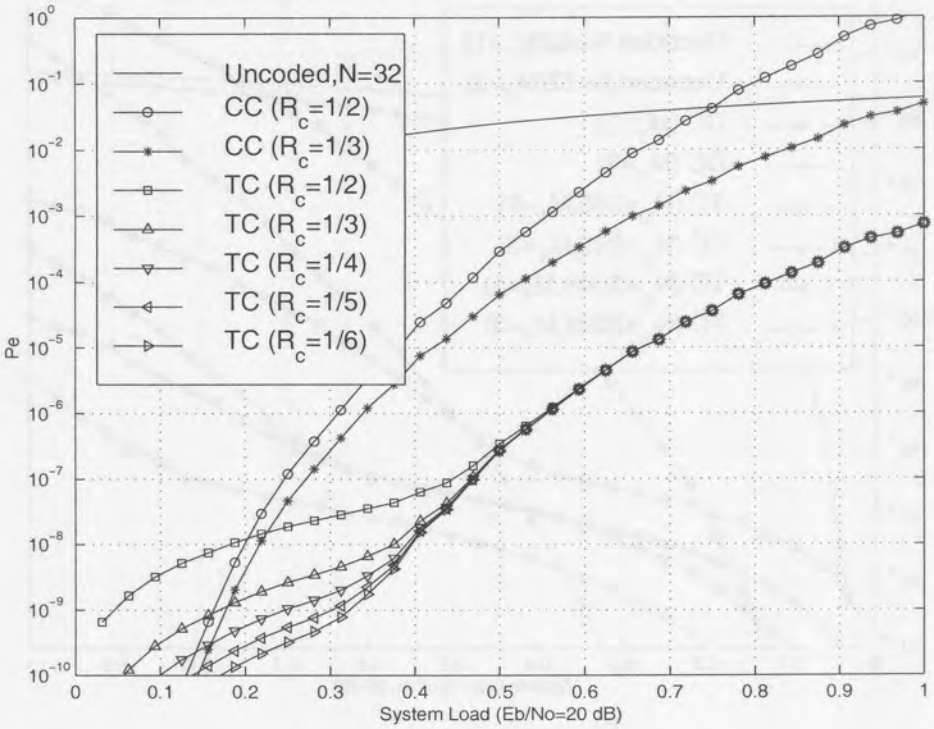

Figure 5.10. Coded O-CDTD BEP performance on a 2-path fading channel with $N_{tc} = 256$ and $M_T = 1$.

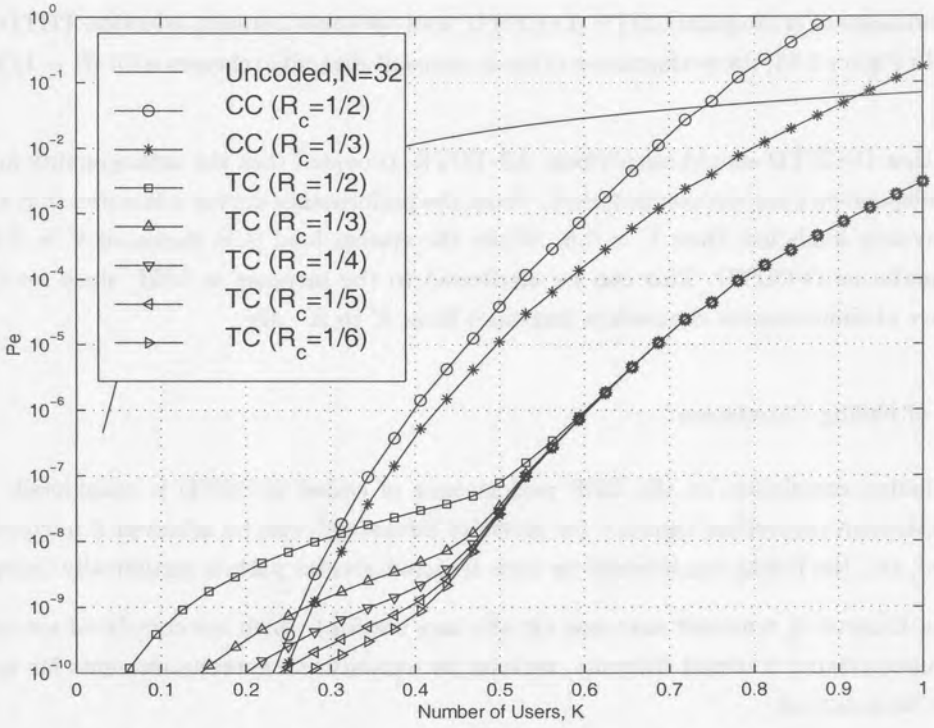

Figure 5.11. Coded O-CDTD BEP performance on a 2-path fading channel with $N_{tc} = 256$ and $M_T = 2$.

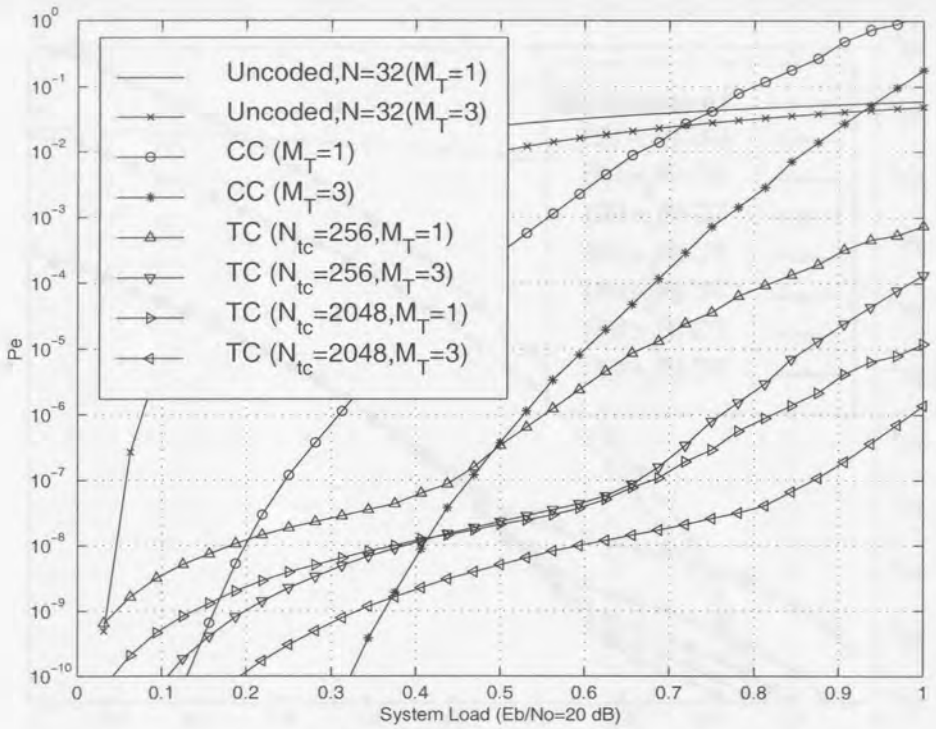

Figure 5.12. Coded O-CDTD performance comparison with $R_c = 1/2$, $N_{tc} = 256, 2048$ and $M_T = 1, 3$.

5.3.2 CDTD and TDTD Comparison

The BEP performance of orthogonal CDTD (O-CDTD) and optimum antenna-selection TDTD (AS-TDTD) is considered. In Figure 5.13, the performance of these transmit diversity schemes with $R_c = 1/2$ and $M_T = 3$ is compared.

It is expected that O-CDTD should outperform AS-TDTD, provided that the orthogonality and conditions of statistical independence are not compromised. From the performance curves it is noted that this argument is correct for system loads less than $V = 0.5$. When the system load is in excess of $V = 0.5$, AS-TDTD signalling outperforms O-CDTD. This can be attributed to the increase in MAI, since for O-CDTD the effective number of simultaneous channels is increased from K to $K \cdot M_T$.

5.3.3 Effects of Fading Correlation

The effect of fading correlation on the BEP performance of coded O-CDTD is considered. It has been argued that maximum theoretical capacity (or diversity advantage) can be achieved if uncorrelated signals are transmitted, i.e., the fading experienced by each transmit-receive path is statistically independent.

As explained in Chapter 3, transmit antennas (at the base station) which are correlated are considered. In order to have uncorrelated transmit diversity, we have to separate the antenna elements far apart ($\approx 40\lambda$), which may not be practical.

To investigate the influence of correlation, Figure 5.14 depicts the O-CDTD performance with $R_c = 1/2$, $M_T = 3$, and constant fading correlation coefficients, $\rho = 0.0, 0.5$ and 0.99. The performance degradation due to correlation is not that significant if ρ is restricted to 0.5. However, the performance is severely

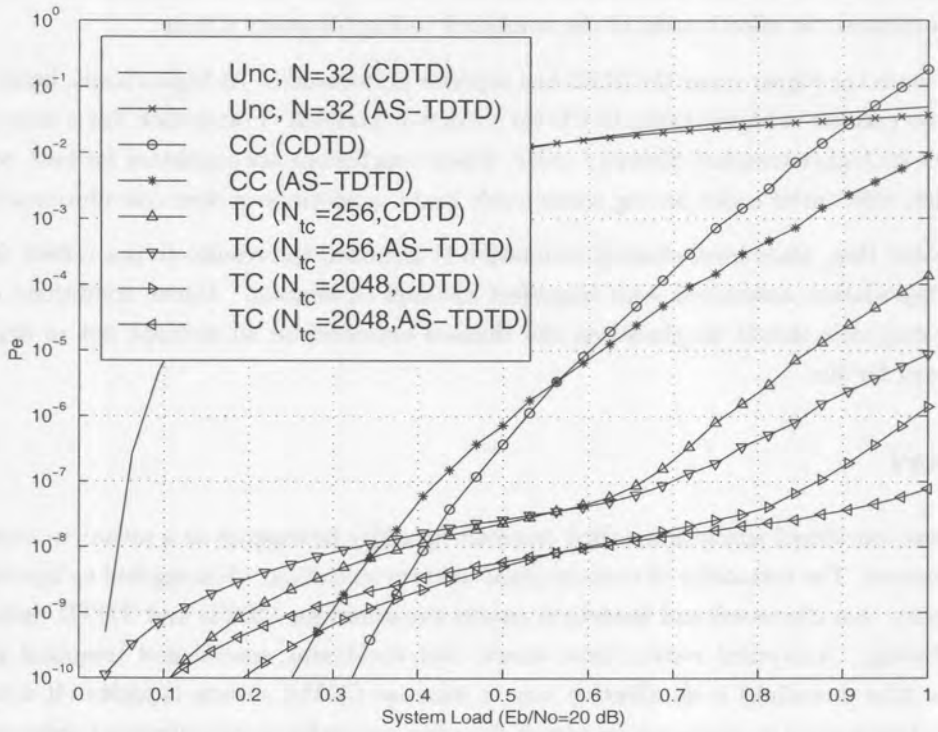

Figure 5.13. Comparison of $R_c = 1/2$ convolutional and turbo coding ($N_{tc} = 256, 2048$) CDTD and AS-TDTD.

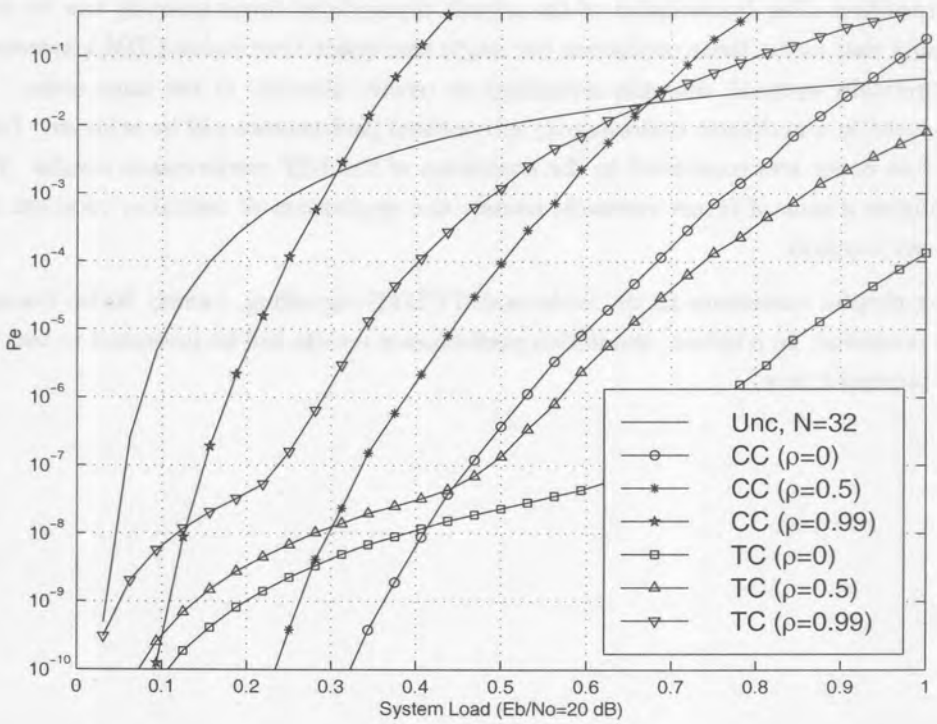

Figure 5.14. Comparison of $R_c = 1/2$ convolutional and turbo coding ($N_{tc} = 256, 2048$), with $M_T = 3$ and $\rho = 0, 0.5, 0.99$.

degraded when $\rho \geq 0.5$. The latter can be attributed to the fact that the correlated multi-path channel has memory which reduces the effectiveness of the combined coding/diversity scheme.

At low system loads the higher order O-CDTD has superior performance. At higher loads, however, the MAI increases and no gain for a higher order O-CDTD scheme is possible. Correlation has a more pronounced degrading effect for higher transmit diversity order. These conclusions are consistent for both convolutional- and turbo codes, with turbo codes having consistently better performance than convolutional codes.

It should be noted that, since ideal channel estimation is assumed, the results do not reflect the additional performance degradation associated with imperfect channel estimation. Under conditions of correlated fading, strong emphasis should be placed on the channel estimator in an attempt not to degrade system performance even further.

5.4 SUMMARY

This chapter has considered space-time coded transmit diversity techniques as a means to improve cellular CDMA performance. The suitability of convolutional- and turbo coding, when applied to layered space-time transmit diversity, was discussed and analytical results presented for CDTD and TDTD under conditions of multipath fading. Analytical results have shown that combining spatial and temporal processing at the transmitter (the downlink) is an effective way to increase CDMA system capacity. It was shown that turbo coding, when applied to space-time transmit diversity, outperforms convolutional codes with the same code rate and comparable complexity. In general, the average performance of the CDTD and TDTD is comparable.

It was argued that when orthogonal spreading is combined with the multiple transmit antennas the destructive superposition after combination of the signals transmitted simultaneously can be avoided. It is important to note that under these conditions the single user space-time coded CDMA system will achieve the same, theoretically optimal, diversity advantage as receive diversity of the same order. When a MF receiver is employed in a multiuser environment, sub-optimal performance will be achieved. For this reason the use of random codes was considered in the derivation of the BEP performance results. The foregoing argument highlights a area of future research, namely the application of multiuser receivers in the coded transmit diversity scenario.

In the following chapter extensions to the turbo coded CDTD signalling, namely turbo transmit diversity (TTD) will be presented. In addition, simulation performance results will be presented to test the goodness of the bounds presented here.

6 SPACE-TIME TURBO CODED TRANSMIT DIVERSITY

In the foregoing chapter the superior performance achieved with space-time turbo coded CDTD systems have been presented. In this chapter extensions to layered space-time coding are considered. In this chapter different turbo transmit diversity (TTD) scenarios are considered. The classification of the three TTD scenarios is illustrated in Figure 6.1. These are parallel concatenated turbo transmit diversity (PCTTD) [216, 217, 218], serial concatenated turbo transmit diversity (SCTTD)[1] [219], and super-orthogonal turbo transmit diversity (SOTTD) [220, 221, 222].

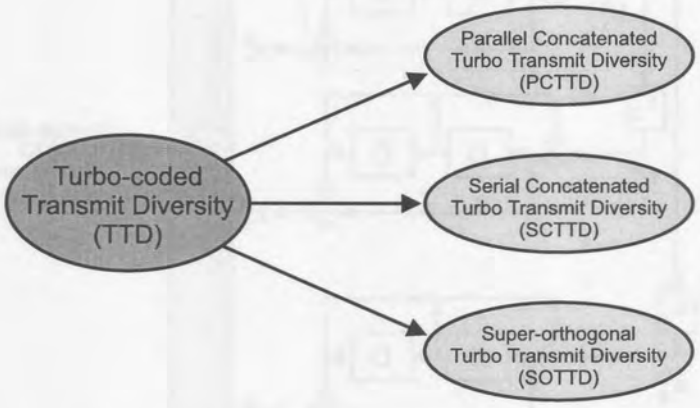

Figure 6.1. Turbo transmit diversity space.

Both PCTDD and SCTTD offer a sub-optimal, but practical implementation of the turbo coded CDTD system. The principle of operation is to transmit the coded bits, stemming from the constituent encoders, via the spatial domain rather than via the time, code or frequency domain. The received data stream is then iteratively decoded using turbo decoding principles. The way the turbo coder is configured fits naturally into the CDTD schemes described in the previous chapter.

SOTTD provides a flexible architecture for the generation of variable low rate coded transmit diversity. Here, techniques of spreading and coding at low-rate are married with the code-division transmit diversity and iterative "turbo" processing. In very general terms SOTTD can be considered as a special case of orthogonal turbo-coded CDTD, employing codes of very low rate.

Detail concerning the design, realization and BEP performance of the three TTD scenarios will be presented in the following sections.

6.1 PARALLEL CONCATENATED TURBO TRANSMIT DIVERSITY (PCTTD)

In the layered space-time turbo coded CDTD signalling, a turbo encoder (and its associated iterative decoder) is required for every transmit diversity branch available. In PCTDD a single turbo encoder-decoder pair is required, with the only requirement being that the number of constituent RSC encoders Z, should be greater or equal to the transmit diversity order M_T. By applying appropriate puncturing the original single antenna rate $R_c = 1/2$ code is transformed into a more powerful space-time rate $R_c = 1/(Z+1)$ code. The way the turbo coder is configured fits naturally into the transmit diversity schemes described above.

PCTTD can be implemented as orthogonal or non-orthogonal CDTD, and is an novel extension of the work by Barbalescu [223]. The principle of operation is to transmit the coded bits, stemming from the constituent RSC encoders, via the spatial domain rather than via the time, code or frequency domain. The received data stream is then iteratively decoded using turbo decoding principles. The power of PCTTD lies in the principle that a single-antenna rate $R_c = 1/2$ coder is transformed into a more powerful turbo code with rate $R_c = 1/(Z+1)$, where Z is the number of constituent encoders as shown in Figure 6.2.

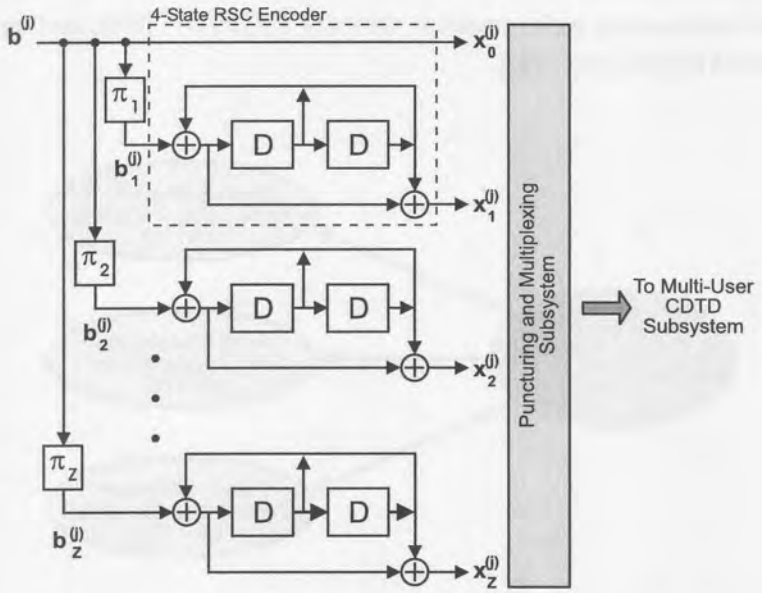

Figure 6.2. Generalized block diagram of PCTDD encoder.

The PCTTD scheme is based on three underlying principles. These are the

- rate $R_c = 1/(Z+1)$ turbo encoding,
- puncturing and multiplexing, and

- the iterative decoding.

These principles are described in detail below.

6.1.1 Rate-$1/(Z+1)$ Turbo Encoding

The constituent turbo encoder of Figure 6.2 produces one uncoded output systematic stream $\mathbf{x}_0^{(j)}$ and Z encoded output parity streams, denoted by $\mathbf{x}_1^{(j)}, \ldots, \mathbf{x}_Z^{(j)}$. Here

$$\mathbf{x}_Z^{(j)} = \{x_{0,z}^{(j)}, x_{1,z}^{(j)}, x_{2,z}^{(j)}, \ldots, x_{i,z}^{(j)}, \ldots, x_{(N_{tc}-1),z}^{(j)}\}, \ (z = 0, 1, \ldots, Z), \tag{6.1}$$

where i is the discretized time index, and j denotes the reference user. The parity streams are produced by Z identical RSC encoders with constraint length L_{tc}. In the discussion that follows the constrained length $L_{tc} = 3$.

The first component encoder operates directly (or through interleaver π_1) on the information sequence, $\mathbf{b}_1^{(j)}$ of length N_{tc}, producing two output sequences $\mathbf{x}_0^{(j)}$ and $\mathbf{x}_1^{(j)}$. The second component encoder operates on a re-ordered sequence of information bits, $\mathbf{b}_2^{(j)}$, produced by interleaver π_2, also of length N_{tc}, and outputs the sequence $\mathbf{x}_2^{(j)}$. The systematic information bit stream of this RSC encoder is discarded. Subsequent component encoders operate on a re-ordered sequence of information bits, $\mathbf{b}_Z^{(j)}$, produced by interleaver π_Z, and output the sequence $\mathbf{x}_Z^{(j)}$.

6.1.2 Puncturing and Multiplexing

The puncturing and multiplexing procedures form the heart of PCTTD. As an example, to show how a rate $R_c = 1/2$ code is being transformed into a rate $R_c = 1/(Z+1)$ code by appropriate puncturing and multiplexing, consider a turbo encoder with Z constituent RSC encoders and a single transmit antenna $M_T = 1$. Assuming further for our example QPSK modulation, the information and coded sequences of user j can be arranged in terms of the in-phase and quadrature phase components. The in-phase component of the QPSK modulator (I branch) transmits the systematic bits, while the quadrature component (Q branch) transmits the parity bits formed by the constituent encoders. Beginning at discrete time $i = 0$, the in-phase component is modulated by

$$I: \left\{x_{0,0}^{(j)}, x_{1,0}^{(j)}, \ldots, x_{(Z-1),0}^{(j)}, x_{Z,0}^{(j)}, x_{(Z+1),0}^{(j)}, \ldots, x_{(N_{tc}-2),0}^{(j)}, x_{(N_{tc}-1),0}^{(j)}\right\}, \tag{6.2}$$

while the quadrature component is modulated by

$$Q: \quad \left\{x_{0,1}^{(j)}, x_{1,2}^{(j)}, \ldots, x_{(Z-1),Z}^{(j)}, x_{Z,(Z+1)}^{(j)}, x_{(Z+1),(Z+2)}^{(j)}, \cdots, x_{(N_{tc}-2),(Z-1)}^{(j)}, x_{(N_{tc}-1),Z}^{(j)}\right\}. \tag{6.3}$$

This puncturing and multiplexing procedure is illustrated in Figure 6.3(a), using the notation $x_{i,Z}^{(j)}$. It should be pointed out that, due to the puncturing procedure, some of the coded sequences are not transmitted to maintain the $R_c = 1/2$ coding rate.

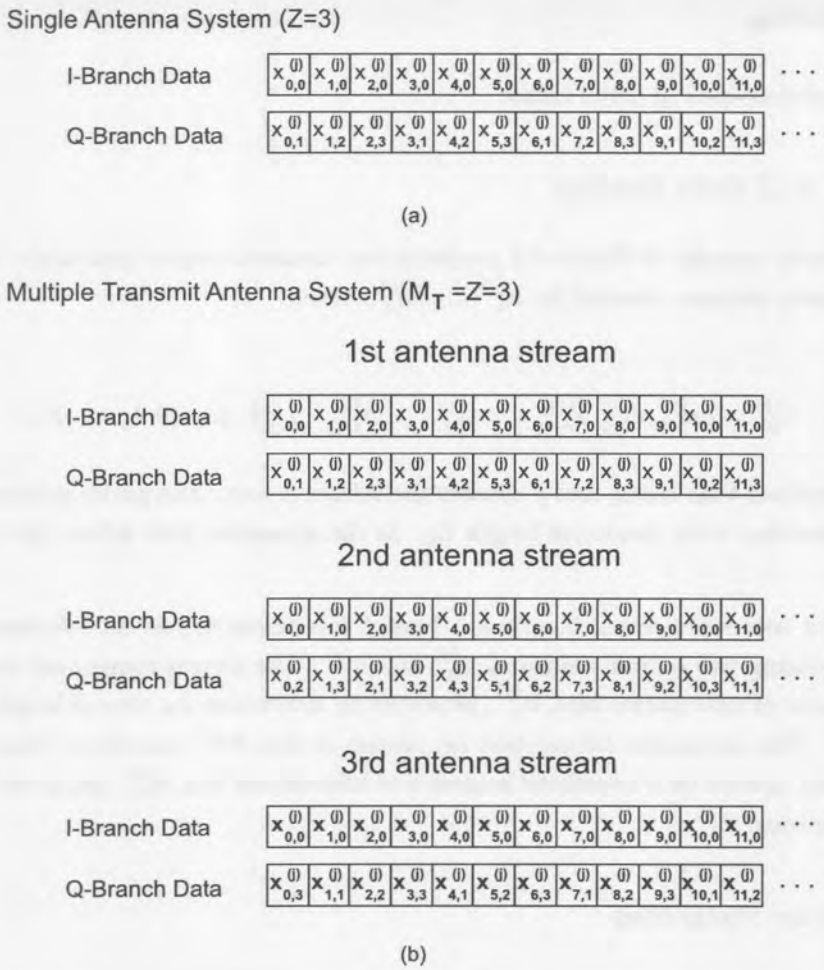

Figure 6.3. Puncturing and multiplexing procedure for a rate $R_c = 1/2$ turbo encoder with Z constituent RSC encoders. (a) Single transmit antenna, $M_T = 1$ (b) $M_T = 3$ transmit antennas.

The single transmit antenna $M_T = 1$ example can easily be extended to $M_T = Z$ transmit antennas. In PCTTD with $(M_T > 1)$, the systematic information sequences are repeatedly transmitted on the I branches of all the available transmit antennas. This is done to guarantee soft failure in order to achieve maximum space-time diversity gain. In addition, smart puncturing and multiplexing is employed to assign the parity information sequences to the different Q branches available for transmission. This puncturing and multiplexing procedure is shown in Figure 6.3(b) for $M_T = Z = 3$. Note that the information and coded sequences transmitted by the I and Q branches of the first antenna element for $M_T > 1$, agrees with the single antenna transmission of Figure 6.3(a).

The I and Q sequences transmitted by the second antenna can be written as

$$\begin{aligned} I: &\quad \left\{x_{0,0}^{(j)}, x_{1,0}^{(j)}, \cdots, x_{Z,0}^{(j)}, x_{(Z+1),0}^{(j)}, \cdots\right\} \\ Q: &\quad \left\{x_{0,2}^{(j)}, x_{1,3}^{(j)}, \cdots, x_{(Z-2),Z}^{(j)}, x_{(Z-1),1}^{(j)}, x_{Z,2}^{(j)}, \cdots\right\}. \end{aligned} \tag{6.4}$$

In general, the sequences transmitted by the zth antenna element can be written as

$$
\begin{aligned}
I: &\quad \left\{x_{0,0}^{(j)}, x_{1,0}^{(j)}, x_{2,0}^{(j)}, x_{3,0}^{(j)}, x_{4,0}^{(j)}, x_{5,0}^{(j)}, \cdots\right\} \\
Q: &\quad \left\{x_{0,z}^{(j)}, x_{1,(z+1)}^{(j)}, \cdots, x_{(Z-z-1),Z}^{(j)}, x_{(Z-z),1}^{(j)}, \cdots\right\}.
\end{aligned} \tag{6.5}
$$

It should be noted that none of the encoded information bits are lost by the puncturing and multiplexing operations, while the effective transmission per constituent QPSK transmission rate remains one half.

6.1.3 *Iterative Decoding*

Figure 6.4 depicts the iterative decoding configuration. Before the decoding is performed, the demodulated signal streams are de-multiplexed. For the punctured symbols values are obtained from the $Z-1$ received antenna streams. For a PCTTD system with $M_T < Z$, zero values are inserted in the punctured bit positions. The decoder therefore regards the punctured bits as erasures.

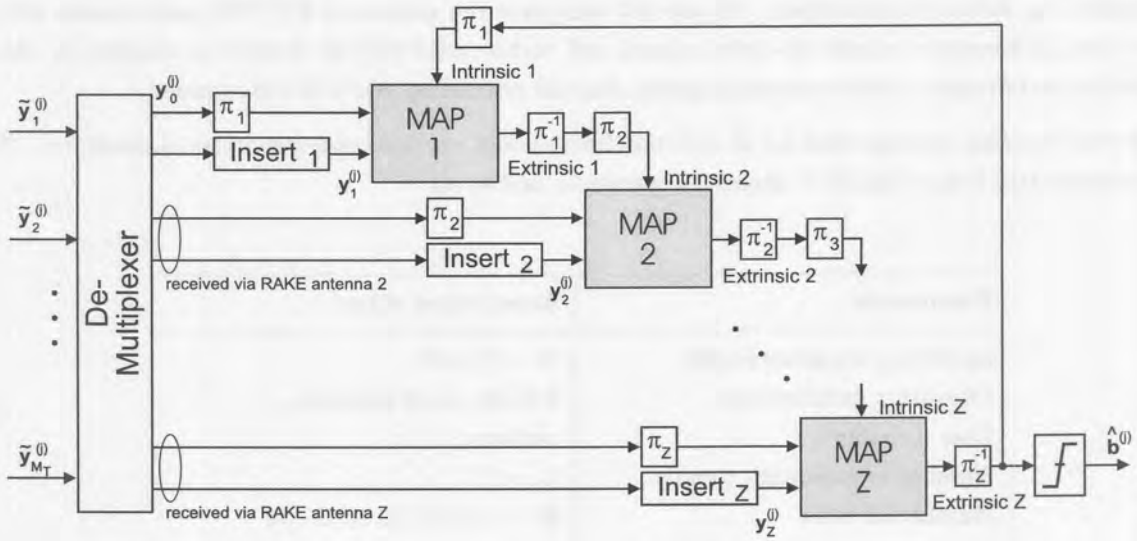

Figure 6.4. Generalized block diagram of PCTTD decoder operating in the serial mode.

From our previous single antenna PCTTD example, the following sequences are inputs to the zth decoder

$$
\begin{aligned}
I: &\quad \left\{y_{0,0}^{(j)}, y_{1,0}^{(j)}, \cdots, y_{Z,0}^{(j)}, y_{(Z+1),0}^{(j)}, \cdots\right\} \\
Q: &\quad \left\{y_{0,z}^{(j)}, 0, 0, \ldots, 0, y_{Z,z}^{(j)}, \cdots\right\}.
\end{aligned} \tag{6.6}
$$

The iterative decoding procedure requires Z component decoders using soft inputs and providing soft outputs, based on the MAP algorithm. The decoding configuration operates in *serial mode*, i.e. decoder 1 processes data before decoder 2 starts its operation, and so on [224]. Many different configurations exist, especially for the case where $Z \geq 3$.

With reference to Figure 6.4, extrinsic information (related to a data symbol) is obtained from surrounding symbols in the codeword sequence imposed by the code constraints only. The extrinsic information is obtained without any information concerning the symbol itself, and is provided as soft outputs by the

component decoders. The soft outputs, obtained from the MAP, are internal variables of the decoder, and is a measure of the reliability of the decoding of single bits and do not provide hard bit decisions.

In addition, intrinsic information related to a data symbol is *a priori* information attached to the symbol without using any code constraints. This information is used by the component decoders as additional information related to each code symbol. In iterative decoding, the extrinsic information provided by the previous decoding step becomes the *a priori* information of the current decoding process.

6.1.4 *Performance Considerations*

In this section the performance of the proposed PCTTD scheme is considered. Since PCTTD exhibits the closest resemblance to turbo coded CDTD, the performance of PCTTD should be compared with that of the turbo coded CDTD signalling. Monte-Carlo simulations are conducted to verify the goodness of the BEP bounds presented in Chapter 5.

Using the system parameters outlined in Table 6.1, the BER performance of a PCTTD CDMA has been determined by means of simulation. Figure 6.5 compares the simulated PCTTD performance with the theoretical performance bounds of convolutional and turbo coded CDTD derived in Chapter 5. For the simulation performance perfect synchronization, channel estimation and CSI are assumed.

The turbo decoding configuration for $Z = 3$ constituent codes operates operates in serial mode, i.e., "MAP 1" processes data before "MAP 2" starts its operation, and so on.

Parameter	**Simulation value**
Spreading sequence length	$N = 32 \times R_c$
Operating environment	2-Path, equal strength.
User distribution	uniform
Number of multipath signals	$L_p = 2$
Number of users	$K = 1, 5, 10, 15, 20, 25, 30$
Number of RAKE fingers	$L_R = 2$
PCTTD Parameters	
Transmit antenna elements	$M_T = 1, 3$ $\rho = 0$
Code rate	$R_c = 1/2$
Constituent encoders	$Z = 3$
Interleaver	S-type, $N_{tc} = 256$
Decoder	Iterated MAP, serial configuration.

Table 6.1. System parameters for BER simulation of PCTTD.

Concentrating on the BER curves of the PCTTD system, slight disparities between the simulation results and performance bounds can be identified for target BER of 10^{-6} or worse. As can be seen from the curves, the simulation curves are very close the the simulation bounds, for normalized user loads less than 0.75. For the conditions of low load ($P_b < 10^{-6}$), the performance of the simulated system is dominated by the performance of the sub-optimal (non ML) decoder and practical interleaver utilized.

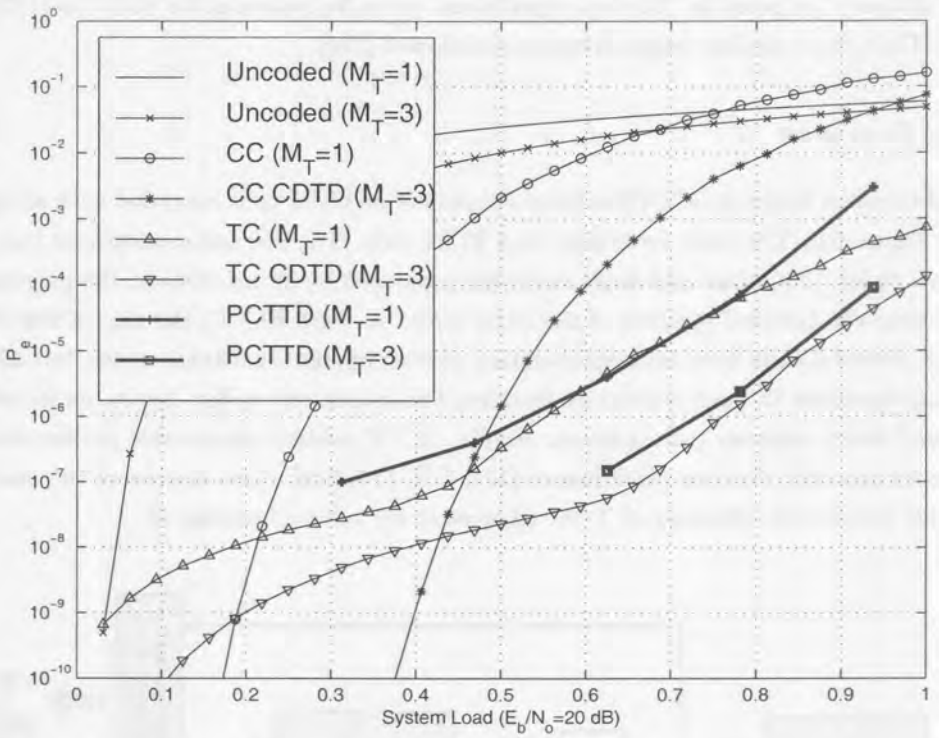

Figure 6.5. Performance comparison of the simulated BER performance of PCTTD and theoretical BEP of CDTD, as a function of the normalized system load, with operating point of $E_b/N_o = 20$ dB.

For the higher load conditions, the simulation results are also worse of than the bounding performance. From the discussion presented in Section 4.2.3, this is attributed to the fact that at low value of SNR, the PCCC bounds resulting from the use of the binomial cpdf should actually be considered as a lower bound to the code's performance. This is a matter of concern when target BER of 10^{-3} and worse. However, most practical systems operate in the BER target range of 10^{-8} (data) to 10^{-3} (voice).

6.2 SERIAL CONCATENATED TURBO TRANSMIT DIVERSITY (SCTTD)

This section deals with the natural extension of the parallel concatenation approach to the SCCTD scenario. SCCCs have drawn interest recently as the serial analogues of turbo codes, which are PCCC. The performance of the SCCC is dominated by terms with an input Hamming weight from the inner code equal to the free distance of the outer code. Many authors have concluded that these terms are made up of the concatenation of inner decoder error events with information weight 2, and it is the Hamming distance of these error events, the "effective free distance", which should be minimized.

Later in this section performance bounds for SCTTD are derived and used to conduct a search for rate-1/2 coded QPSK employing a dual-transmit antenna ($M_T = 2$) signalling scenario. In general, the SCTTD can be extended to accommodate any number of transmit antennas.

In [172] design criteria for SCCC has been developed based on the performance bounds for SCCC. These criteria were used as the basis for code searches to find the best constituent codes for SCCC. The authors of [172] conclude that the outer code in a SCCC should be a traditional convolutional code with as large a free distance as possible, and that the inner code should be a recursive convolutional code with as large an

"effective free distance" as possible. The best constituent codes for proposed for SCCC in [172], will also be optimal for SCTDD, since similar design criteria are followed [219].

6.2.1 *Encoder Description*

The basic dual-transmit antenna SCCTD scheme consists of an outer code cascaded with an inner code, as depicted in in Figure 6.6. The inner code may be a TCM code. The discussion presented here is restricted to convolutional codes. The inner and outer codes are separated by an interleaver, the purpose of which is to permute in time the encoded symbols of the outer code. As with PCCC, the aim of the SCCC scheme is to generate a powerful code from the concatenation of two simpler constituent codes, but which admits a simple decoding algorithm through separately decoding the constituent codes. Again, an iterative decoding algorithm is used which achieves near-optimum results. SCCC achieve comparable performance to PCCC, and in some cases can offer superior performance [172, 173, 174, 175]. Also, the use of the inner TCM code allows the higher bandwidth efficiency of TCM schemes to be taken advantage of.

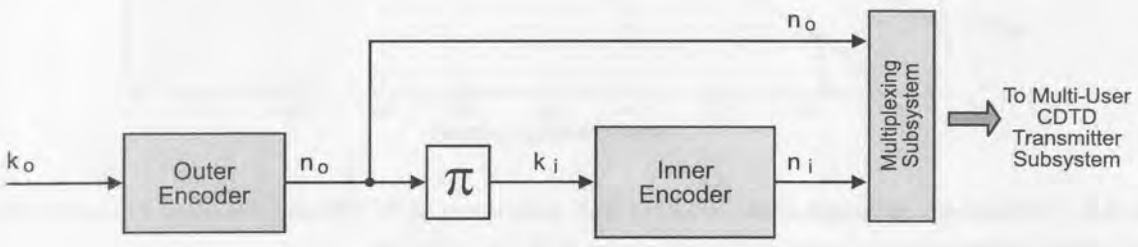

Figure 6.6. Generalized block diagram of SCTDD encoder.

The encoder for a SCCC is depicted in Figure 6.6. Both encoders are convolutional codes; the outer encoder has rate $\frac{k_o}{n_o}$ and the inner encoder has rate $\frac{k_i}{n_i}$. The information bits are encoded by the outer encoder and the resulting code bits are interleaved by the bit-wise random interleaver (π) and become the information bits of the inner encoder. This interleaver applies an N_{tc} bit random permutation to the sequence of code bits coming from the outer encoder. There is a corresponding de-interleaver in the decoder, and both the interleaver and de-interleaver must be synchronized. This means that, as in the case of PCCC and PCTTD, some form of framing information header must be transmitted. The most straight-forward implementation of a SCCC is with frames of information bits which, after encoding by the outer encoder, are equal in size to the interleaver. As for PCCCs the SCCC can be analyzed as a block code, with a code word with $N_{tc}\,\frac{k_o}{n_o}$ information bits and $N_{tc}\,\frac{n_i}{k_i}$ code bits [175]. The overall SCCC code rate is $\frac{k_i}{n_i}\,\frac{k_o}{n_o}$. It is usual, although not essential, to have $n_o = k_i$, resulting in an overall code rate of $\frac{k_o}{n_i}$.

As in single antenna SCCC, the interleaver is an essential feature of the SCCTD scheme, and the performance improves with increasing N_{tc}. However, as the interleaver is random, the transmission of the codeword cannot commence until the interleaver has been filled, and decoding cannot be completed until the entire codeword is received. The PCCC encoding latency was N_{tc} information bits, but the SCCC encoding latency is $N_{tc}\,\frac{k_o}{n_o}$ information bits, due to the action of the outer code. This results in an overall latency of $2\,N_{tc}\,\frac{k_o}{n_o}$ information bits (plus propagation delay and decoding delay). This difference in latency between PCCC and SCCC means that two schemes should be compared not with identical interleaver sizes, but with identical latency.

In [172, 175] it is concluded that the inner constituent code of a SCCC scheme should be a RSC code and that of the outer constituent code should be a traditional convolutional with maximum free distance. It

is also concluded that the effective free distance of the inner code should be maximized, and as such the constituent codes found for PCCC can be used as the inner codes of a SCCC scheme.

6.2.2 *Decoder Description*

The near-optimal iterative decoding structure for the PCTTD scheme can be readily adapted for the decoding of SCTTD scheme. In the decoder structure for the SCTTD the soft outputs of the inner code bits from the demodulator are decoded to produce soft decisions of the inner information bits. These are, after de-interleaving, also the soft decisions of the outer code bits. These are in turn decoded to produce improved soft decisions of the outer code bits, which, when interleaved, are improved soft decisions of the inner information bits. This process is iterated a number of times, before finally the outer decoder produces a hard decision of the outer information bits.

Both the inner and outer encoders are "connected" to the channel, the M_T outputs of the demodulator along with an estimate of the noise variance are used to calculate the probabilities of the code symbols for both the inner and outer codes. The decoder output corresponding the to first antenna is input to the inner MAP module, along with the interleaved code symbol probabilities of the outer code from the previous iteration (because outer code symbols are inner information symbols). Only the updated inner code information symbol probabilities are used, which is de-interleaved to become the outer code code symbol probabilities. The outer code code symbol probabilities are interleaved and input to the inner code MAP module during the next iteration, and, if it is the final iteration, the updated outer code information symbol probabilities is used to make the final decision.

6.2.3 *Performance of SCCC*

Consider the concatenation of two linear convolutional constituent codes C_o and C_i, joined by a bit-wise random interleaver defined by the permutation π. The outer code C_o has rate $R_o = k/p$ and the inner code C_i has rate $R_i = p/n$, resulting in an overall SCCC with rate $R_c = k/n$. The interleaver is of length N, which is an integer multiple of p (actually, the inner and outer codes can have rates $R_i = k_i/n_i$ and $R_o = k_o/n_o$, respectively, constraining the interleaver length to $N_{tc} = \text{lcm}(n_o, k_i)$. However, this complicates the bound expressions and is not considered here). The block size of the SCCC is NR_o bits.

There are N_{tc} interleavers of length N_{tc}, many of which will yield different performance when used in the SCCC. Rather than exhaustively enumerating the performance for all possible interleavers, an uniform interleaver is assumed. Any interleaver will permute an input word with Hamming weight h into an output word which also has Hamming weight h, and there are $\binom{N_{tc}}{h}$ of such permutations.

If the trellis is terminated at both the beginning and the end of a frame then the weight enumerating function (WEF) of the constituent codes can be determined from the equivalent block code. In the case of continuous transmission and decoding the analysis is much more complex. It involves the use of a hyper-trellis having as hyper-states pairs of states of the outer and inner codes. Each hyper-branch represents all the paths taken through both the inner and outer trellises for one interleaver block. Each hyper-branch represents all the paths taken through both the inner and outer trellises for one interleaver block. The WEF for each hyper-branch can be determined by treating the constituent codes as equivalent block codes, starting and finishing at these known states. The upper bound to the BEP can then be found by applying the standard transfer function bound approach [16] to the hyper-trellis.

However, for codes with a reasonable number of states and for large interleavers this technique becomes prohibitively complex. In [174] an approximation is introduced which is accurate when the interleaver

length is larger than the constituent code's memory. This approximation involves replacing the complete transfer function of the hyper-trellis by the WEF which labels the hyper-branch joining the zero states of the hyper-trellis. This of course is the WEF found from the equivalent block codes of the constituent codes when they both start start and finish in the all-zero state. This means that for the case of continuous transmission and decoding an accurate approximation to the bit error probability bound is that of the case of a terminated trellis.

Define the WEF of any code C as

$$A^C(I,D) = \sum_{i,d} A^C_{i,d}\, I^i\, D^d, \tag{6.7}$$

a polynomial in the dummy variables I and D, where $A^C_{i,d}$ is the number of codewords of C with input Hamming weight i, and output Hamming weight d. WEFs can also be expressed for all codewords with input Hamming weight i, and for all codewords with Hamming weight d.

The WEFs of the outer and inner constituent convolutional codes, $A^{C_o}(I,D)$ and $A^{C_i}(I,D)$, can be found from knowledge of their respective trellises [225]. Any specific codeword of C_o with output Hamming weight h will, through the action of the uniform interleaver, generate a codeword of C_i of input Hamming weight h with probability $1/\binom{N_{tc}}{h}$. There are a total of $A^{C_o}_{i,h}$ of these codewords with input Hamming weight i in C_o, and a total of $A^{C_i}_{h,d}$ of these codewords with input Hamming weight d in C_i. Thus the total number of codewords of the SCCC with input Hamming weight i and output Hamming weight d is

$$A^C_{i,d} = \sum_{h=0}^{N_{tc}} \frac{A^{C_o}_{i,h} \times A^{C_i}_{h,d}}{\binom{N_{tc}}{h}}. \tag{6.8}$$

The upper bound to the BEP of the SCCC is [174]

$$P_b \leq \sum_{i=1}^{NR_o} \sum_{d=1}^{N_{tc}/R_i} A^C_{i,d}\, \frac{i}{2\, N_{tc}\, R_o}\, Q\left(\sqrt{d\, R_o\, R_i\, \frac{E_b}{N_o}}\right). \tag{6.9}$$

For large interleavers this expression will contain a very large number of terms, however it can be evaluated more quickly by only including those terms which make a significant contribution to the bound, i.e., the d summation may be truncated.

6.2.3.1 The WEF of the Equivalent Block Code. The coefficients $A^{C_o}_{i,h}$ and $A^{C_i}_{h,d}$ of the equivalent blocks codes to the constituent convolutional codes can be found by concatenating the error events of the convolutional codes. The error events of the convolutional codes can be found by modifying the techniques of [225] to allow remergings with the all-zero state. Let $T(L,I,D,J)$ be the transfer function of the convolutional code which enumerates all paths in the trellis remerging with the zero state at or before step M, with possible remergings with the zero state for just one step before this.

$$T(L,I,D,J) = \sum l,i,d,j\; T_{l,i,d,j} L^l\, I^i\, D^d\, J^j\,, \tag{6.10}$$

where $T_{l,i,d,j}$ is the number of paths in the trellis of length l, input Hamming weight of i, an output Hamming weight of d, and j remergings with the zero state (i.e., the concatenation of j error events). The codewords of the equivalent block code can be determined by observing that each error path of length l and number of remergings j gives rise to $\binom{M-l-j}{j}$ codewords [174].

The weight enumerating coefficients of the equivalent block code are given by [174]

$$A^C_{l,D} = \sum_j \binom{M-l-j}{j} T_{l,i,d,j} \ . \tag{6.11}$$

By defining

$$T_{i,d,j} = \sum_l T_{l,i,d,j} \ , \tag{6.12}$$

and noting that $\binom{M-l-j}{j} \approx \binom{M}{j}$, the coefficient $A^{C_o}_{i,h}$ of the outer code can be approximated by

$$A^{C_o}_{i,h} \approx \sum_j \binom{N_{tc}/p}{j} T^{C_o}_{i,h,j} \ , \tag{6.13}$$

and the coefficient $A^{C_i}_{h,d}$ of the inner code can be approximated by

$$A^{C_i}_{h,d} \approx \sum_j \binom{N_{tc}/p}{j} T^{C_i}_{h,d,j} \ , \tag{6.14}$$

recall that $p = n_o = k_i$.
Using (6.8) the weight enumerating coefficient of the SCCC is then

$$A^C_{i,d} \approx \sum_{h=d^o_H}^{N_{tc}} \sum_{j^o} \sum_{j^i} \frac{\binom{N_{tc}/p}{j^o}\binom{N_{tc}/p}{j^o}}{\binom{N_{tc}}{h}} T^{C_o}_{i,h,j^o} T^{C_i}_{i,h,j^i} \ , \tag{6.15}$$

where d^o_H is the free Hamming distance of the outer code.

This expression can be simplified further by using the asymptotic approximation to the binomial coefficient for large M,

$$\binom{M}{m} \approx \frac{M^m}{m!} \ . \tag{6.16}$$

Substituting (6.16) and (6.15) into (6.9) yields

$$Pb \leq \sum_d D_d \, Q\left(\sqrt{d \, R_o \, R_i \, \frac{E_b}{N_o}}\right) \ , \tag{6.17}$$

where

$$D_d = \sum_{i=1}^{N_{tc}\,R_o} \sum_{h=d_H^o}^{N_{tc}} \sum_{j^o} \sum_{j^i} \frac{i}{2\,N_{tc}\,R_o} N_{tc}^{j^o+j^i-h-1} \frac{h}{p^{j^o+j^i}\,j^o!j^i!} T^{C_o}_{i,h,j^o}\,T^{C_i}_{i,h,j^i}\,. \tag{6.18}$$

For large N_{tc} the dominant coefficient of d will be the one for which the exponent of N_{tc} is maximum. Define this maximum exponent for each d as

$$\alpha(d) = \max_{i,h}\{j^o + j^i - h - 1\}\,. \tag{6.19}$$

In [172] design criteria for SCCC are developed by examining both the overall maximum of the exponent given in (6.19), and the value of the exponent corresponding to minimum output Hamming weight h. The maximum exponent allows the dominant contribution to P_b to be found as $N_{tc} \to \infty$. The exponent for the minimum weight allows the BEP to be evaluated as $E_b/N_o \to \infty$.

6.2.3.2 SCCC design criteria. In this paragraph the design criteria for SCCC is revisited.

Outer code. From the discussions presented in [172, 175], the outer code should have as large a free distance as possible. This will be achieved with a non-recursive convolutional code. In general, the SCCC BEP bound is dominated by error events for which $h = d_H^o$, i.e., error event from the inner decoder which generate errors in the outer code with Hamming weight equal to the free distance of the outer code. In addition, as $E_b/N_o \to \infty$ the performance of the SCCC will be dominated by the minimum value of d in the bound, which is the free distance of the SCCC.

Inner code. The authors of [175] conclude that the inner code in a SCCC should be chosen to be recursive, and to have as large a Hamming weight as possible for a weight 2 input codeword.With a recursive convolutional inner code there are error events with $h = d_H^o$ which are more likely than this. Thus the inner convolutional code in an SCCC should be designed to minimise the contribution of error events with $h = d_H^o$. This is the same criteria used for PCCC, and the codes found in [176] can be used.

Interleaver. A random bit-wise interleaver should be used. As with PCCC, S-type random interleavers give best performance with SCCC. The interleaver should be as large as possible. As with PCCC this latency means that in delay sensitive applications, such as voice transmissions, a trade-off must be made between delay and performance.

6.2.4 SCTTD Performance Approximation

The performance of a rate 1/3 SCTTD CDMA system with $M_T = 2$ antennas is considered. The system parameters outlined in Table 6.2 are assumed. The general system parameters, e.g., spreading length, are similar to the parameters given in Table 6.1.

The outer code is a 4-state rate 1/2 non-systematic convolutional code taken from [14] (Table 11.1(c)), with generator polynomials $g_1 = 5_8$ and $g_2 = 7_8$. The minimum Hamming distance of this code is 5. The inner code is a 4-state rate 2/3 RSC code taken from [176] (Table 1), with generator polynomials $h_0 = 7_8$, $h_1 = 3_8$ and $h_2 = 5_8$. The minimum Hamming weight for a weight 2 input word for this code is 4.

Parameter	Simulation value
PCTTD Parameters	
Transmit antenna elements	$M_T = 1, 2$ $\rho = 0$
Code type and rate	
Outer Code	4-state, $R_c = 1/2$
Inner Code	4-state, $R_c = 2/3$
Effective Code Rate	$R_c = 1/3$
Interleaver	Uniform , $N_{tc} = 256$

Table 6.2. System parameters for numerical evaluation of BEP performance.

Using (3.29), (4.6), (6.17), (6.18), and the system parameters outlined in Table 6.2, the approximate BEP performance of the SCTTD cellular CDMA system can been determined numerically. The results are shown in Figure 6.7.

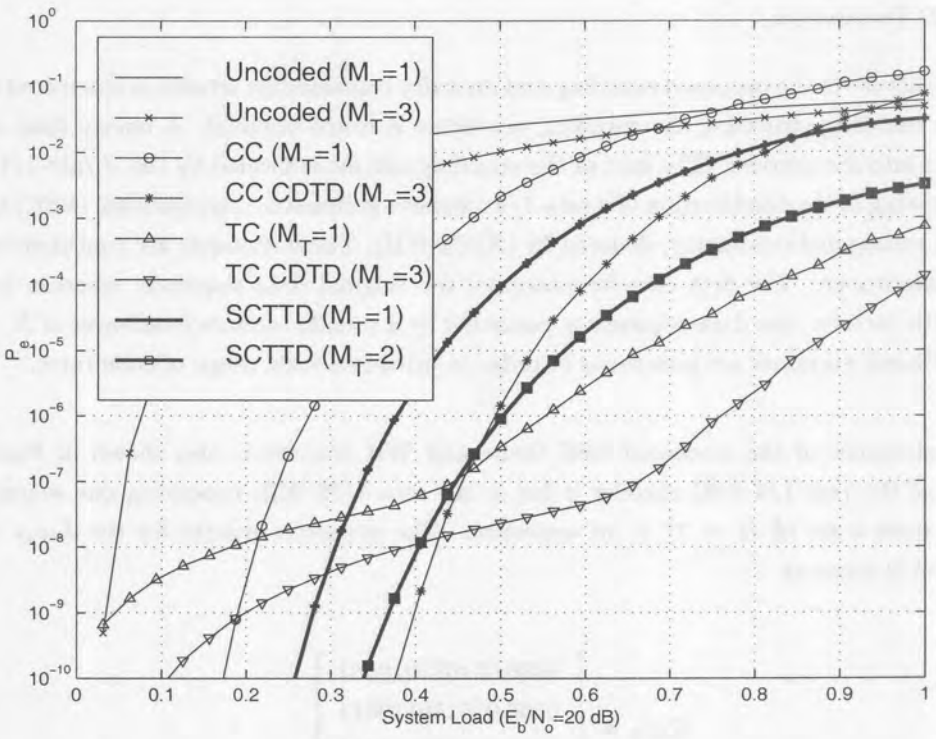

Figure 6.7. BEP performance of SCTTD as a function of the normalized system load, with operating point of $E_b/N_o = 20$ dB.

Shown on the figure are the performance of single and $M_T = 2$ transmit diversity systems' performance. The performance degradation of SCTDD system as opposed to the turbo coded CDTD (essentially PCTTD) system at average to high system loads is evident. The promising effect is the excellent performance exhibited at low system loads, implying that given a large interleaver, excellent performance may be achieved over

the complete user range. As interleaver size (gain), however, increases so does decoding delay, and thus a balance must be found between acceptable performance and tolerable latency.

6.3 SUPER-ORTHOGONAL TURBO TRANSMIT DIVERSITY (SOTTD)

This section presents the SOTTD signaling scenario for spread-spectrum CDMA communication systems. SOTTD extends layered turbo coded transmit diversity to include Z component decoders, and is roughly based in the work by Pehkonen *et al.* [42, 43]. The techniques of spreading and coding at low-rate are married with the code-division transmit diversity and iterative "turbo" processing [222]. The principle of operation is to transmit the coded bits, stemming from the constituent encoders, via the spatial domain rather than via the time and code domain. The received data stream is then iteratively decoded using turbo decoding principles.

A synchronous CDMA mobile communications system is considered where the transmitter is equipped with M_T antennas at the base station and a single receiving antenna at the mobile. The signals on the matrix channel, i.e. the $M_T \times 1$ transmission paths between transmitter and receiver, are supposed to undergo independent frequency selective Rayleigh fading. It is assumed that the path gains are constant during one frame and change independently from one frame to another (quasi-static fading).

6.3.1 SOTTD Transmitter

The general structure of the proposed encoding and diversity transmission scheme is illustrated in Figure 6.8. Owing to this encoding structure, the encoding procedure is frame oriented. A binary data sequence $\mathbf{b}$ of length N is fed into the encoder. The hart of the encoding scheme is formed by the Z rate-1/16 constituent encoders, consisting of the combination of a rate-1/4 recursive systematic convolutional (RSC) encoder and a rate-4/16 WH orthogonal modulator, denoted by (RSC&WH). These encoders are concatenated in parallel applying an interleaver. The first encoder processes the original data sequence, whereas before passing through the Zth encoder, the data sequence is permuted by a pseudo random interleaver of N. The outputs of the Z constituent encoders are punctured in order to provide a wide range of code rates.

The detailed structure of the combined RSC turbo and WH encoder is also shown in Figure 6.8. The state outputs of the rate-1/4 RSC encoder is fed to the rate-4/16 WH, producing one sequence of length ($L_{WH} = 16$) from a set of $H = 2^4 = 16$ sequences. The generator matrix for the $L_{WH} = 16$ WH in systematic form is given as

$$G_{WH} = \begin{bmatrix} 1000\,011011010101 \\ 0100\,010110110011 \\ 0010\,001110001111 \\ 0001\,000001111111 \end{bmatrix}$$

Recall from coding theory, that the most important characteristic of a codeword is its minimum free distance. Owing to the orthogonality characteristics of the WH codewords, the minimum distance of the encoded sequences for both constituent encoders is equal to $d^{WH} = L_{WH}/2 = 8$. In addition, full-rank transmit diversity may be achieved provided that the transmit antennas are sufficiently spaced.

After encoding, the output sequences are obtained by appropriate puncturing according to puncturing patterns $P^{(i)} = \{p_1^i, p_2^i, \ldots, p_N^i\}$, where $i = 1$ and 2, for the first and second puncturer, respectively. With

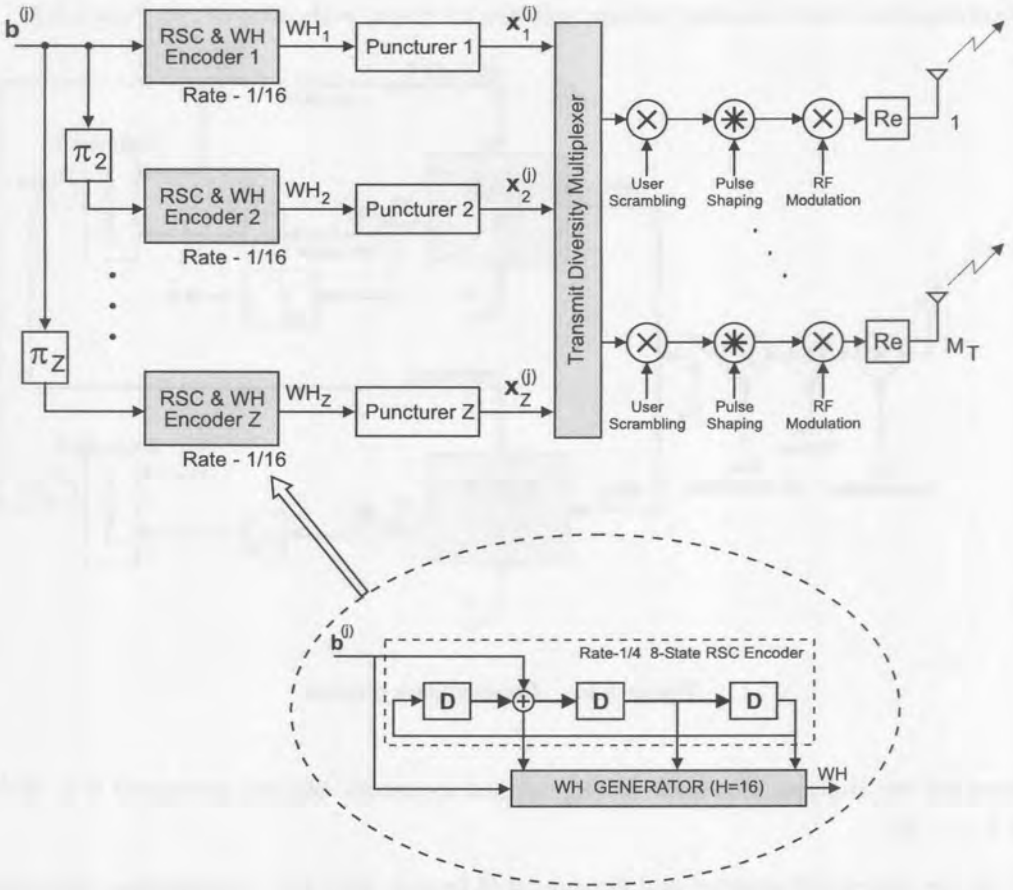

Figure 6.8. Transmitter block diagram.

$W_{P(1)}$ and $W_{P(2)}$, the weights of the first and second puncturers, respectively, the resulting overall encoder rate (R_c) is given by:

$$R_c = \frac{1}{W_{P(1)} + W_{P(2)}} \tag{6.20}$$

Therefore, for the case when none of the output sequences' bits are punctured the overall code rate of the combined turbo and WH encoding strategy is given as $R_c = 1/(16+16) = 1/32$.

After encoding, the Z encoded streams are multiplexed to the M_T available transmit antenna section, encapsulating the user specific scrambling, spreading and chip shaping.

6.3.2 SOTTD Receiver and Iterative Decoder

For description a dual transmit, $M_T = 2$ and single receive antenna, $M_R = 1$ system is assumed. Without loss of generality, the number of constituent encoders Z is taken as 2, i.e. $M_T = Z = 2$. Figure 6.9 shows general receiver for the SOTTD system, as well as the iterative turbo decoding strategy.

Before the actual decoding takes place, for those bits that were punctured, zero values are inserted. Therefore the decoder regards the punctured bits as erasures. The iterative decoding of the turbo coding scheme requires two component decoders using soft inputs and providing soft outputs. The soft output Viterbi algorithm (SOVA) or maximum *a posteriori* (MAP) algorithm may be employed.

Detail concerning the actual decoding process will now be given, with reference to Figure 6.9.

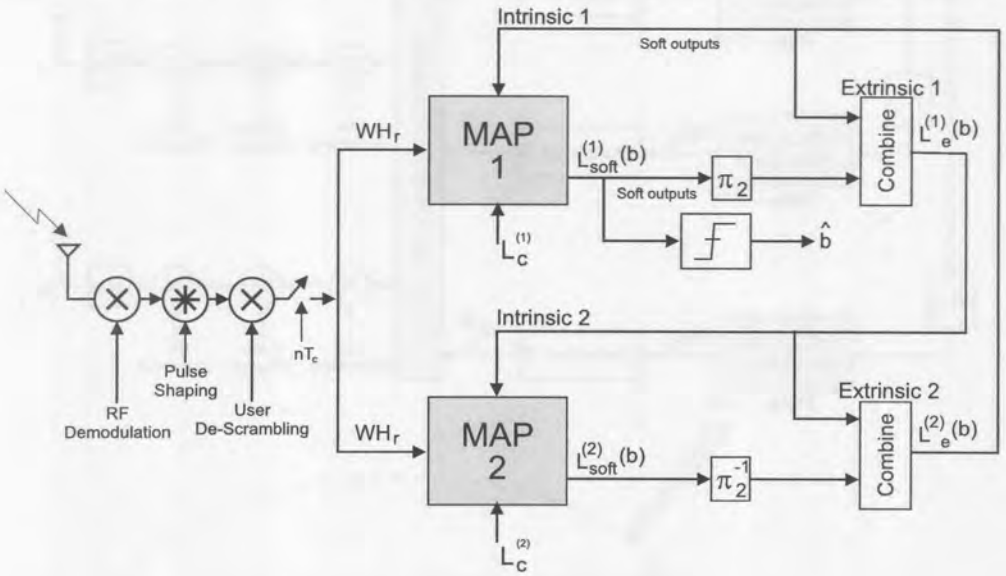

Figure 6.9. Receiver block diagram.

It is assumed for the analysis, that none of the encoded sequences' bits are punctured (i.e., $WH_z = \bar{WH}_z$, where $i = 1, \ldots, Z$).

Let WH_r be the associated received and demodulated branch with the corresponding reliability values of the channel, $L_c^{(z)}$, $z = 1, 2$, depending on whether decoder 1 or 2 is being used. The decoder accepts a priori values $L_i(b)$ for all the information bit sequences and soft-channel outputs $L_c^{(z)} \cdot WH_r$

The branch metric calculation is performed very efficiently by using soft-output inverse WH (SO-IWH) transformation, which basically correlates the received WH sequence with the branch WH sequences terminating in a specific node. Then, by discarding the branch with the lowest accumulated path metric, the maximum likelihood branch is retained.

The soft-input soft-output delivers *a posteriori* soft outputs $L(\hat{b})$ for all the information bits and extrinsic information $L_e(b)$, which for the current bit is only determined by its surrounding bits and the code constraints. It is therefore independent of the intrinsic information and the soft output values of the current bit. It is important to note that all the above mentioned sequences are vectors of length $L_{WH} = 16$.

Ideally, the log-likelihood ratio (LLR) soft-output of the decoder for the information bit b is written as

$$L(\hat{b}) = (L_c \cdot WH_r + L_i(b)) + L_e(\hat{b}) \tag{6.21}$$

implying that there are three independent estimates, which determine the LLR of the information bits: the a priori values, $L_i(b)$, the soft-channel outputs of the received sequences $L_c \cdot WH_r$, and the extrinsic LLR's $L_e(\hat{b})$.

At the commencement of the iterative decoding process there usually are no a priori values $L_i(b)$, hence the only available inputs to the first decoder are the soft-channel outputs obtained during the actual decoding process.

After the first decoding process the intrinsic information on b is used as independent[2] *a priori* information at the second decoder. The second decoder also delivers *a posteriori* information, which is used to derive the extrinsic information, which is – for its part – used in the subsequent decoding process at the first decoder in the next iteration step. The final decision is, of course, based on the *a posteriori* information, output from the second decoder. Note, that initially the LLRs are statistically independent, however, since the decoders use indirectly the same information, the improvement through the iterative process becomes marginal, as the LLR's become more and more correlated.

6.3.3 *Points to Ponder*

Various authors have stated that the design of a optimal interleaver helps to avoid low weights of encoded sequences in many cases, which leads to improved bit error rate performance. In our context, the weight of the encoded sequences (excluding the all-zeros codeword) also equals $d^{WH} = 8$. This is an important observation since it removes the requirement to design an optimal interleaver. For this reason a simple pseudo random interleaver is utilized.

The size of the interleaver, however, and not its design (for our application), determines the performance of the coded system. The larger the interleaver size (N), the larger the "interleaver gain" and greater the potential to increase the temporal spread of successive bits of the original data sequence.

It is important to note that the constituent RSC&WH encoders may produce similar WH codewords. Since these codewords are transmitter over different antennas the full-rank characteristic of the system is still guaranteed. Under multipath fading scenarios, some of the orthogonality will be destroyed. The latter is not a function of the specific WH codeword transmitted at the different antennas, but rather dependent on the delay spread of the channel. Transmitting the same WH codewords over the different antennas will have an effect on the channel estimation and initial system synchronization procedures.

The performance of the SOTTD system depends not on the distance properties of the WH code, but actually on the distance properties of the combined RSC&WH code. In this context, the most important single measure of the code's ability to combat interference is d_{min}.

Figure 6.10 depicts the modified state diagram of the RSC&WH constituent code under consideration. The state diagram provides an effective tool for determining the transfer function, $T(L, I, D)$, and consequently d_{min} of the code. The exponent of D on a branch describes the Hamming weight of the encoder corresponding to that branch. The exponent of I describes the Hamming weight of the corresponding input word. L denotes the length of the specific path.

Through visual inspection the minimum distance path, of length $L = 4$ can be identified as: $a_0 \rightarrow c \rightarrow b \rightarrow d \rightarrow a_1$. This path has a minimum distance of $d_{min} = 4 \times d^{WH} = 32$ from the all-zero path, and differs from the all-zero path in 2 bit inputs.

6.3.4 *Performance Evaluation*

In this section it is attempted to shed some light on the theoretical comprehension of parallel concatenated WH codes. In particular, an upper bound to the average performance of the parallel concatenated codes, stemming from characteristics of the combined RSC&WH (where $L_{WH} = 32$) constituent code, will be defined and evaluated.

Given an (n, k) RSC&WH constituent code, C_z, its input redundancy weight enumerating function (IRWEF) is given by [174]:

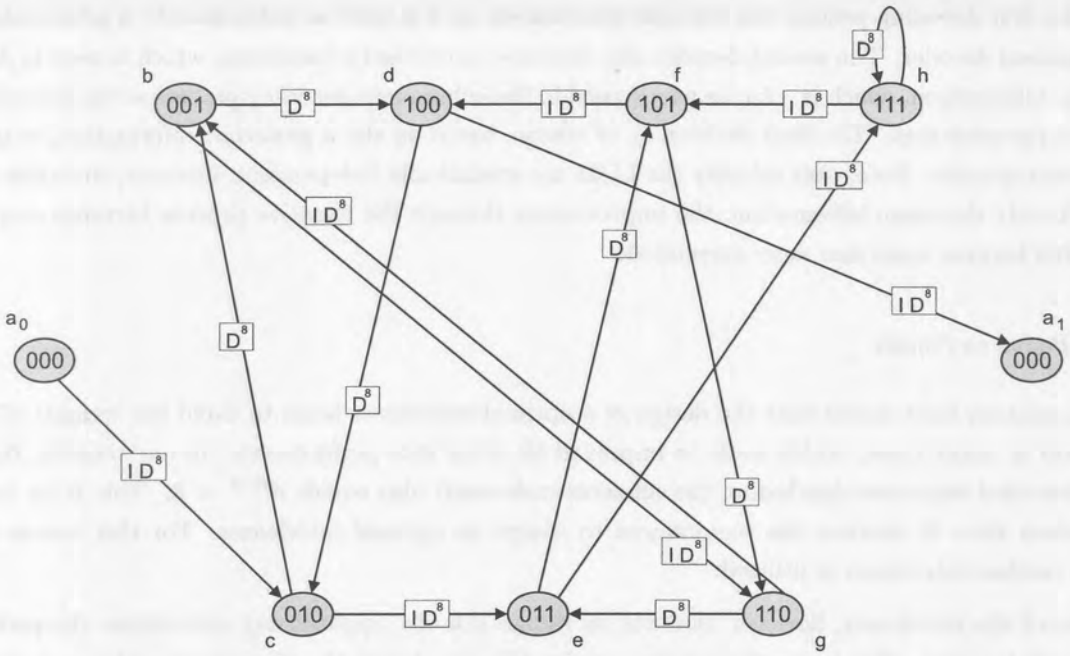

Figure 6.10. Trellis diagram of RSC&WH constituent encoder.

$$A^{C_z}(I,D) \doteq \sum_{i,d_p} A_{i,d_p} I^i D^{d_p}, \tag{6.22}$$

where A_{i,d_p} is the integer number of codewords generated by an input word with Hamming weight i whose parity check bits have Hamming weight d_p. Therefore, the overall Hamming weight is $d = i + d_p$. The IRWEF characterizes the whole encoder, as its depends on both the input information words and codewords.

The IRWEF makes implicit in each term of the normal weight enumerating function (WEF) the separate contributions of the information and the parity-check bits to the total Hamming weight of the codewords.

When the contributions of the information and redundancy bits to the total codeword weight is split, the IRWEF for the constituent WH code is obtained as

$$A^{C_z}(I,D) = 1 + 4ID^7 + 6I^2D^2 + 4I^3D^5 + I^4D^4 \tag{6.23}$$

When employing a turbo interleaver of length kN, the IRWEF of the new constituent (nN, kN) code C_z^N is given by

$$A^{C_z^N}(I,D) = \left[A^{C_z}(I,D)\right]^N, \tag{6.24}$$

for all Z the constituent codes.

Using (6.24) the conditional WEF, $A_i^{C_z^N}(D)$ of the constituent codes can be obtained from the IRWEF as

$$A_i^{C_z^N}(D) = \frac{1}{i!} \cdot \frac{\delta^i A^{C_z^N}(I,D)}{\delta I^i}\bigg|_{I=0}. \tag{6.25}$$

From the conditional WEF, owing to the property of the uniform interleaver of length kN, the conditional WEF of the two-constituent ($Z = 2$) parallel concatenated code of length $((2n - k)N, kN)$ is obtained as

$$A_i^{C_P^N}(D) = \frac{A_i^{C_z^N} \cdot A_i^{C_z^N}}{\binom{kN}{i}}. \tag{6.26}$$

The IRWEF of the parallel concatenated code using the the following inverse relationship can be obtained as

$$A^{C_P^N}(I, D) = \sum_i I^i A_i^{C_P^N}(D). \tag{6.27}$$

To compute an upper bound to the bit error probability (BEP), the IRWEF can be used with the union bound assuming maximum likelihood (ML) soft decoding. The BEP, including the fading statistics (assumed to be slow fading), assumes the form

$$\begin{aligned} P_{b|\mathbf{s}} &\leq \frac{I}{k} Q\left(\sqrt{d_{min}\sigma_{0c}\mathbf{s}}\right) \\ &\cdot \; e^{d_{min}\sigma_{0c}\,\mathbf{s}} \cdot \frac{\delta A(I, D)}{\delta I}\bigg|_{I=D=e^{-\sigma_{0c}\mathbf{s}}}, \end{aligned} \tag{6.28}$$

where σ_{0c} denotes the effective signal-to-noise ratio (SNR), and S denotes the power of the received signal.

Assuming that the cellular system is employing omni-directional antennas, the total output SNR term used in (6.27) can be determined as

$$\sigma_{0c} = \left(\frac{1}{R_c}\frac{N_o}{2\,E_b} + \frac{(K \cdot M_T - 1)}{3N}\right)^{-1}. \tag{6.29}$$

Also, if it is assumed that the M_T transmit diversity transmissions are equal powered, with constant correlation between the branches, and transmitted over a Rayleigh fading channel, the components of the received power vector S are identically distributed, with pdf given by

$$\begin{aligned} p_{\mathbf{S}}(\mathbf{s}) &= \frac{1}{\Omega^2\Gamma(M_T \cdot L_R)}\left(\frac{\mathbf{s}}{\Omega^2}\right)^{M_T \cdot L_R - 1} \\ &\times \frac{\exp\left(-\frac{\mathbf{s}}{(1-\rho)\Omega^2}\right) \cdot {}_1F_1\left(1, M_T \cdot L_R, \frac{\rho M_T \cdot L_R \mathbf{s}}{\zeta(1-\rho)\Omega^2}\right)}{\zeta\,(1-\rho)^{(M_T \cdot L_R - 1)}}, \end{aligned} \tag{6.30}$$

with $\zeta = 1 - \rho + \rho M_T \cdot L_R$.

From (6.29), ${}_1F_1(\cdot)$ is the confluent hyper geometric function, Ω^2 is the average received path strength (assumed equal), ρ the correlation between transmit or receive branches, and L_R is the number of RAKE receiver fingers.

Using a finite number of terms in (6.27) transforms the upper bound into the approximation

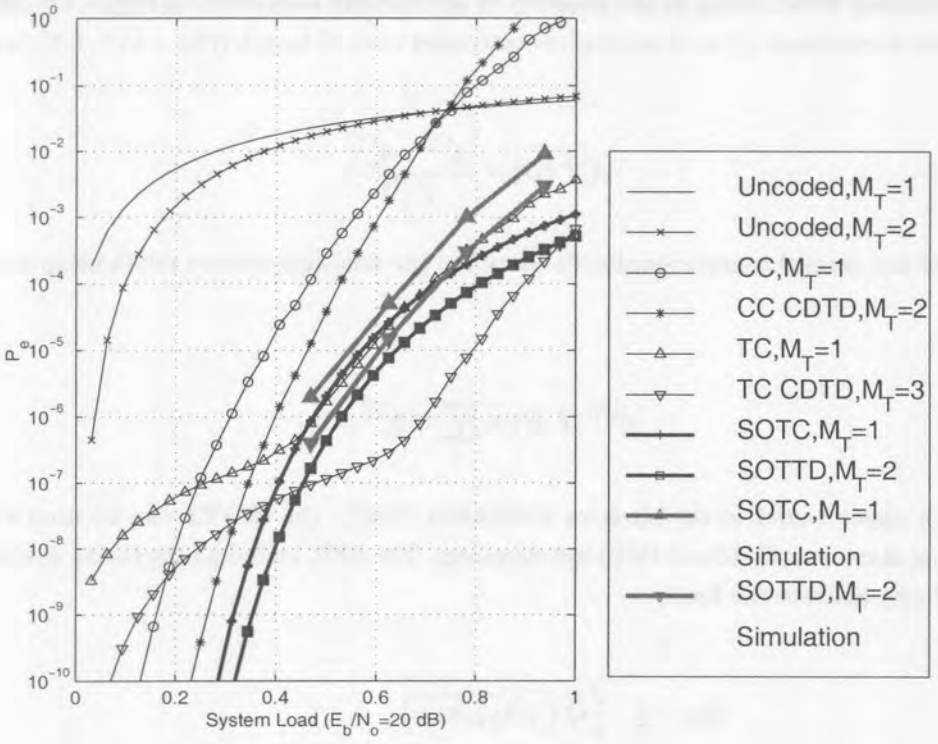

Figure 6.11. Bit error probability as a function of the load (number of users/total spreading), with operating point of $E_b/N_o = 20$ dB.

$$P_{b|\mathbf{S}} \approx \sum_m D_m Q\left(\sqrt{m\sigma_{0c}\,\mathbf{s}}\right), \tag{6.31}$$

where

$$D_m = \sum_{i+d_p=m} \frac{i}{k} A_{i,d_p}, \tag{6.32}$$

where A_{i,d_p} is obtained from the IRWEF of parallel concatenated code (compare (6.22)).

Finally, the BEP is computed using (6.31) and (6.32), when averaged over the fading statistics.

6.3.5 *Analytical and Simulation Results*

The performance of the ($M_T = Z = 2$) super-orthogonal transmit diversity (SOTTD) CDMA system is compared to that of an uncoded, and convolutional- and turbo coded code-division transmit diversity (CDTD) CDMA systems. Table 6.3 presents a summary of the techniques of importance in the performance evaluation.

Using the system parameters outlined in Table 6.4, the BEP performance of a cellular CDMA system employing the different techniques has been determined numerically. The results are shown in Figure 6.11.

Shown on the figure are the performance of single and $M_T = 2, 3$ transmit diversity systems' performance. From the curves it is clear that the superior performance predicted for TC CDTD may achieved with the

Acronym	Definition	Conditions
Uncoded	Uncoded system	$N_{spread} = N = 32$
CC	Convolutional	S=256, $R_c = 1/2$
	Coder	$N_{spread} = N/2$
TC	Turbo Coder	S=4, $R_c = 1/2$
		$N_{spread} = N/2$
SOTC	Super-Orthogonal	S=8, $R_c = 1/32$
	Turbo Coder	$N_{spread} = N/32$
CDTD	Code-Division	Uncoded, CC/TC
	Transmit Diversity	$M_T = 2, 3$
SOTTD	Super-Orthogonal	SOTC
	TTD	$M_T = 2$

Table 6.3. Summary of Techniques.

Parameter	Simulation value
Spreading sequence length	$N = 32 \times R_c$
Operating environment	2-Path, equal strength
User distribution	uniform
Number of MP signals	$L_p = 2$
Number of users	$K = 1, 2, \ldots, N$
Number of RAKE fingers	$L_R = 2$
FEC code type and rate	CC, TC ($R_c = 1/2$)
	SOTC ($R_c = 1/32$)
Turbo Interleaver Length	$N = 256$
TD elements	$M_T = 1, 2, 3$
TD technique	CDTD and SOTTD

Table 6.4. System parameters for numerical evaluation of BEP performance.

SOTTD system over the complete capacity range. Also of importance is the fact that the performance degradation of TC CDTD at low system loads (due to inherent TC error floor), is alleviated by the SOTC system, therefore the superior performance of SOTTD. This is explained in terms of the higher minimum free distance on offer by the rate-1/16 constituent encoders, as opposed to the use of rate-1/2 constituent encoders in turbo coded systems.

6.4 SUMMARY

This chapter has considered layered space-time turbo coded transmit diversity techniques for cellular CDMA. Novel extensions of CDTD have been presented in the form of PSTTD, SCTTD and SOTTD. Analytical performance results for these schemes were presented.

In addition to the three general turbo transmit diversity scenarios discussed in this chapter, many parametric investigations can still be performed. This is necessary to form a complete picture of the performance gains on offer by the different TTD schemes. Some ideas of these future investigations are listed below:

PCTTD. When the number of constituent encoders Z is more than 2, different decoding configurations may be considered. In general the advantage of using more than three or more constituent codes is that the corresponding two or more interleavers have a better chance to break sequences that were not broken by another interleaver. The disadvantage is that, for an overall desired code rate, each code must be punctured more, resulting in weaker constituent codes.

Obvious extensions of the serial mode of decoding are the master-slave, parallel and mixed serial-parallel decoding configurations [176].

SCTTD. It has been shown in [172] that the performance of SCCC schemes can be improved at low SNRs by swapping the inner and outer codes. For instance, rather than using a rate 1/2 outer code and a rate 2/3 inner code, a rate 1/3 SCTTD scheme can be constructed from a rate 2/3 outer code and a rate 1/2 inner code. This arrangement has advantages at low SNRs because the more powerful rate 1/2 code is now decoded first.

The use of non-systematic feed-forward outer convolutional codes have been considered in the SCTTD scheme. However, it is known that systematic feedback codes provide improved performance at low SNRs [226]. Therefore the use of systematic codes as the outer codes of SCTTD schemes may be investigated.

SOTTD. One natural extension to the SOTTD scheme that may be considered, is the use of different spreading sequences. In a typical mobile multiple access communication channel, the multiple access interference experienced by any user in a CDMA system will be complex-valued due to independent phase offsets between signals received from different users. For this reason complex spreading codes may also be employed, in which case the MAI is complex-valued, even without phase offsets, and improved performance can be achieved under practical conditions.

In conclusion, there are a number of important notes which must be made about the performance bounds presented in this chapter and in Chapter 5. These bounds are upper limits on the performance of the codes derived from the use of the union bound. As such the bounds are only valid for the case of ML decoding, and they will diverge significantly from the true performance at low values of E_b/N_o. Also, in practice a sub-optimal decoding algorithm is used which is not ML, and furthermore, the bounds are based upon the uniform interleaver, rather than a real random interleaver. The performance of practical systems is also strongly influenced by the available CSI. Clearly, the lack of CSI shall produce a noticeable degradation in system performance. However, there is much heuristic evidence to suggest that, despite this apparent inconsistency, these bounds do make good design and selection criteria for transmit diversity signalling scenarios.

Notes

1. For sake of notation "cleanliness" in defining the different TTD scenarios, the term serial concatenated turbo transmit diversity is adopted, although the "turbo" term normally refers to parallel concatenation.
2. Interleaving between the two decoders reduces the statistical dependencies effectively.